Journal of Organometallic Chemistry 880 (2019) 196–212

Contents lists available at ScienceDirect

Journal of Organometallic Chemistry

journal homepage: www.elsevier.com/locate/jorganchem

Dendron-functionalized Fe_3O_4 magnetic nanoparticles with palladium catalyzed CN insertion of arylhalide for the synthesis of tetrazoles and benzamide

Mohammad Ali Karimi Zarchi*, Seyed Shahab Addin Darbandizadeh Mohammad Abadi

Department of Organic Chemistry, Faculty of Chemistry, Yazd University, Yazd, P.O. Box 89195-741, Iran

ARTICLE INFO

Article history:
Received 3 August 2018
Received in revised form
22 October 2018
Accepted 2 November 2018
Available online 5 November 2018

ABSTRACT

A novel method for the one-pot synthesis of 5-substituted 1*H*-tetrazoles and Benzamide from arylhalide containing *in situ* CN insertion from inorganic salt source was accomplished in presence of a new magnetically catalyst, palladium on surface-modified Schiff-Base complex. $K_2[Ni(CN)_4]$ plays a role of nontoxic inorganic cyanide source in arylhalide Nucleophilic substitution. The synthesized Pd-Schiff-Base@Fe_3O_4MNPs was characterized by various techniques such as FT-IR, TGA, SEM, VSM, XRD, TEM, ICP-AES, EDX, BET and XPS. The nano structure catalyst was easily recovered by external magnetic field and reused several times without noticeable loss of its catalytic activity. Leaching study of Pd-Schiff-Base@Fe_3O_4 MNPs shows palladium strong bonded to different active parts of catalyst surface. Heterogeneity of this catalyst has been examined using hot filtration and ICP-AES techniques.

1. Introduction

Cascade reactions have fascinated organic chemists due to the their roles in providing the pathways for design the specific targeted molecules of considerable structural and stereochemical complexity poses a significant intellectual challenge and can be one of the most impressive activities in natural product synthesis [1]. High atom economy, economies of labor, time, resource management and waste generated are other undeniable advantages of cascade reactions [2]. As well as, study of cascade reactions is an evergreen field in the branch of organic chemistry due to only a single reaction solvent, workup procedure and purification step.

There are a small number of submitted methods for the synthesis of amides. The reaction of between aldehyde, ammonia and hydrogen peroxide in order the synthesis of Benzamide was reported [3]. Using hydroxylamine source is the other pathway for the synthesis of amides [4].

Tetrazoles are an important class of heterocyclic compounds which attracted significant attention due to the broad spectrum of application in organic synthesis field such as drug design [5], carboxylic acid surrogates, lipophilic spacers [6], antihypertensive [7], anti-allergic [8], antibiotic [9], anti-diabetic [10], anti-arrhythmic [11], anti-inflammatory, anti-neoplastic and antiviral [12,13].

The conventional method for the synthesis of 5-substituted 1*H*-tetrazole is based on [3 + 2] cycloaddition of various nitriles with sodium azide [14,15]. trimethylsilylazide [16], hydroazoic acid [17] and etc. [18–20] are other azide sources. Also, a plethora of catalysts which have been introduced for this type of reaction such as BF_3.OEt [21], $AlCl_3$ [22], Cu_2O [23], ZnO [24], clay [25], TBAF [16], suffer from at least disadvantages such as an unsatisfactory yield, use of toxic solvent and harsh recovery of catalyst.

In recent years, heterogeneous catalysts has attracted increasing interest due to easy recovery of the catalysts and their reusability as two outstanding characteristics [26,27]. In this regard, magnetic nanoparticles (MNPs) have special situation [28]. High surface area, large number of active sites [29–31], high stability, low toxicity, simple separation from the reaction mixture with magnetic forces [32,33], have been attracting attention in various field such as magnetic storage media, biosensing application, medical application such as targeted drug delivery, contrast agents in magnetic resonance imaging (MRI) and magnetic ink for jet printing [34]. Despite the widespread applications of MNPs in diverse field,

* Corresponding author.
E-mail address: makarimi@yazd.ac.ir (M.A. Karimi Zarchi).

https://doi.org/10.1016/j.jorganchem.2018.11.006
0022-328X/

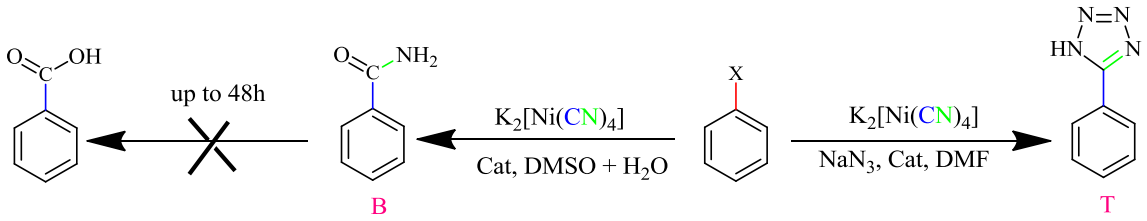

Scheme 1. Synthesis of 5-substituted 1-*H* tetrazole and Benzamide.

particular properties of this bare nanoparticles decreased, because of high aggregation affinity, susceptibility to oxidation, poor morphology and particle size distribution [35–37].

A strategy for solve these problems is utilization silica [38–40], polymer [41–45], carbon [46,47]and precious metals [48,49] for coating these nanoparticles. More importantly, transition metal ions complex of Schiff-Base have been attracted considerable attention due to their various fields of applications such as medicinal, industrial and catalytic activities [50].

Palladium has pivotal role in synthesis of organic compound especially in carbon-carbon coupling field as catalyst [51]. Because of harsh purification of the final products in presence of homogeneous palladium and non-reusability of this catalyst [52–54], heterogeneous palladium was used to overcome on the mentioned problems.

Inspired by importance of cascade reactions and catalytic strategy, herein, we aim to report novel and selective rout for the synthesis of Benzamide and 5-substituted 1*H*-tetrazoles starting from arylhalide in presence of $K_2[Ni(CN)_4]$ as a nontoxic inorganic azide source in the presence of a new magnetically complex, Pd-Schiff-Base@Fe_3O_4MNPs (Scheme 1).

2. Experimental

2.1. Material and struments

All chemicals were commercial products. All reactions were monitored by TLC and yields refer to isolated products. Melting points were obtained on Buchi B-450 apparatus and are uncorrected. ^{1}H and ^{13}C NMR spectra were recorded in DMSO-d_6 on a Bruker AC AV ANCEDPX (400&500) spectrometer. Infrared (IR) spectra of the catalysts and reaction products were recorded on a

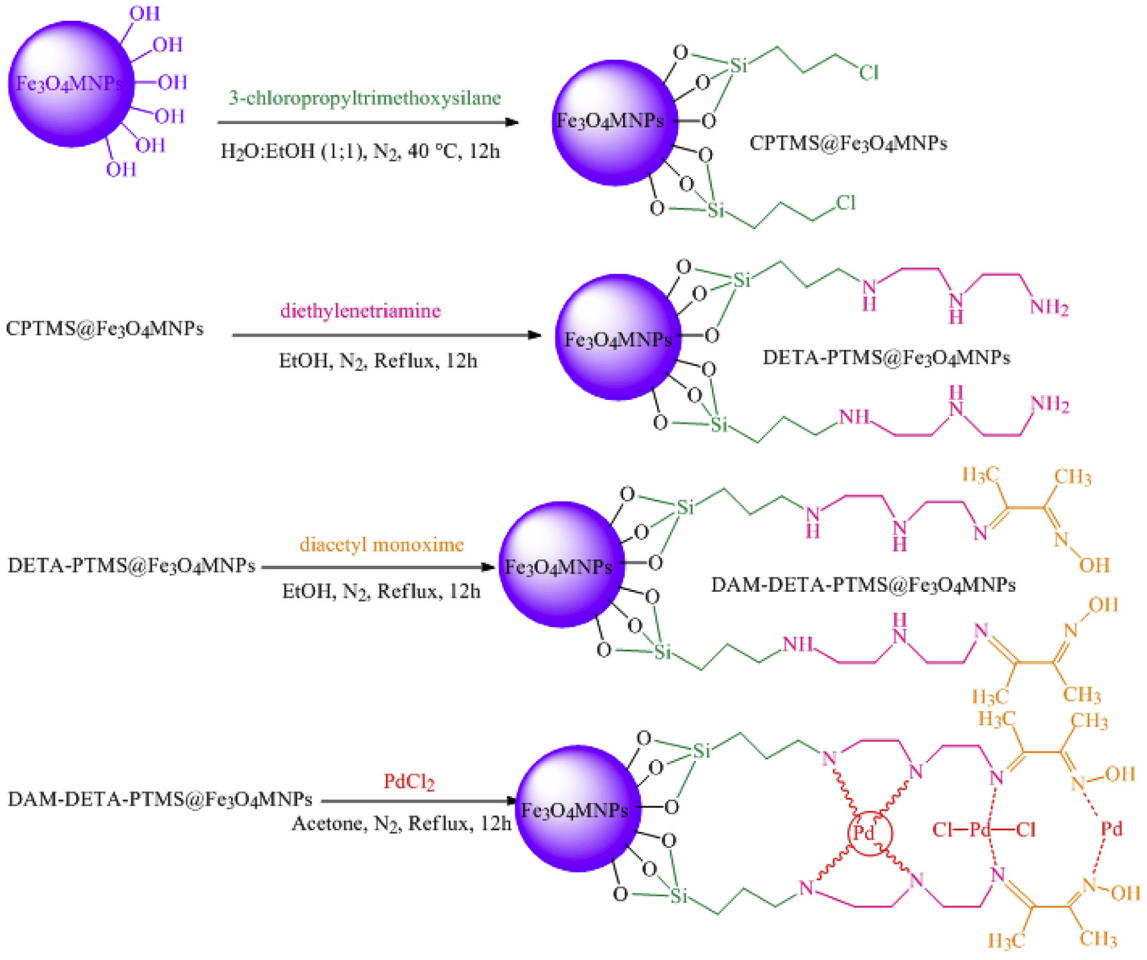

Scheme 2. The plausible structure of Pd-Schiff-Base@Fe_3O_4MNPs

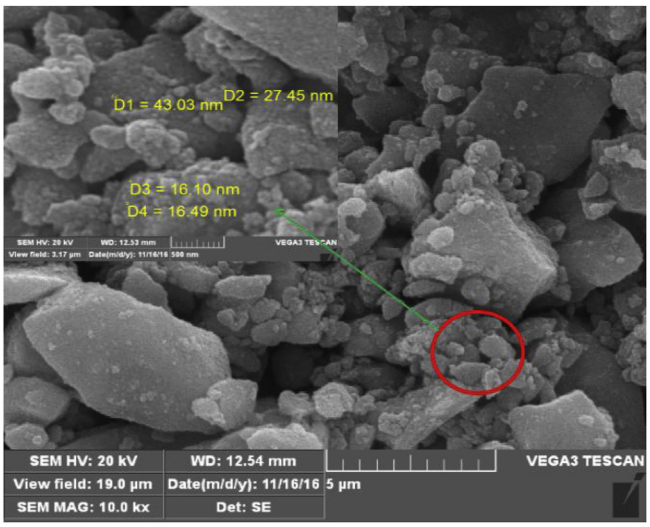

Fig. 1. SEM image of Pd-Schiff-Base@Fe_3O_4MNPs

Bruker FT-IR Equinax-55 single beam spectrophotometer. SEM image was recorded using VEGA3 TESCAN. Transmittance electron microscopy (TEM) image was performed with Ziess-EM10C at 10 KV. XRD pattern was recorded on a panalytical, X'Pert Pro. Amount of palladium carried out with an Analytik Jena nova 300 (model 330, German) atomic absorption spectrometer utilizing an air-acetylene flame atomizer. The thermogeravimetric analysis (TGA) curve is recorded using STA504-germany −BAHR (Ar, up to 1000 °C, 10 °C/min). The specific surface area (BET method), the total pore volume and the mean pore diameter (BJH method) were measured using a N_2 adsorption-desorption isotherm by using a PHS-1020(PHSCHINA) instrument.

2.2. Preparation of Fe_3O_4 magnetic nanoparticles

Fe_3O_4 magnetic nanoparticles was prepared by co-precipitation technique [55]. In a typical procedure, $FeCl_2.4H_2O$ (1.99 g, 10 mmol) and $FeCl_3.6H_2O$ (5.41 g, 20 mmol) were dissolved in Distillated water (30 mL). The solution was heated to 60 °C under nitrogen while being stirred by a mechanical stirrer about 30 min, followed by the slow addition of 25% ammonia solution (35 mL). The mixture was stirred for 30 min. After that, the reaction mixture was cooled then precipitate was separated by external magnet and washed with deionized water (3 × 100 mL). The gel was dried at 80 °C in an oven for 2 h (abbreviated as Fe_3O_4 MNPs).

2.3. Preparation of Schiff-Base complex of Pd on Fe_3O_4MNPs surface

The Schiff-Base complex of Palladium supported on Fe_3O_4 MNPs was prepared as follows. In order to prepare CPTMS@Fe_3O_4MNPs, 1 g of Fe_3O_4 MNPs was dispersed in 50 mL ethanol/water (1:1) solution under ultrasonic irradiation for 60 min afterward, 1.5 mL of 3-chloropropyltrimethoxysilane (CPTMS) was added to the reaction mixture. The reaction mixture was stirred using mechanical stirring under nitrogen atmosphere at 40 °C for 12 h the precipitated was recovered through magnetically separation, washed with ethanol and dried at 80 °C in an oven for 2 h then the resulting solid (CPTMS@Fe_3O_4MNPs) was refluxed with 1 g of diethylenetriamine (DETA) in ethanol for 12 h under nitrogen atmosphere. After this period of time, the reaction mixture was cooled, separated by magnetic decantation, washed with ethanol and dried at 80 °C in an oven for 2 h (abbreviated as DETA-PTMS@Fe_3O_4MNPs). In order to prepare DAM-DETA-PTMS@Fe_3O_4, 0.5 g of diacetyl monoxime was refluxed with DETA-PTMS@Fe_3O_4 in ethanol for overnight under nitrogen atmosphere. The solid product (DAM-DETA-PTMS@Fe_3O_4MNPs), was obtained by magnetically separation, then washed with ethanol and dried by mentioned method. Finally, for

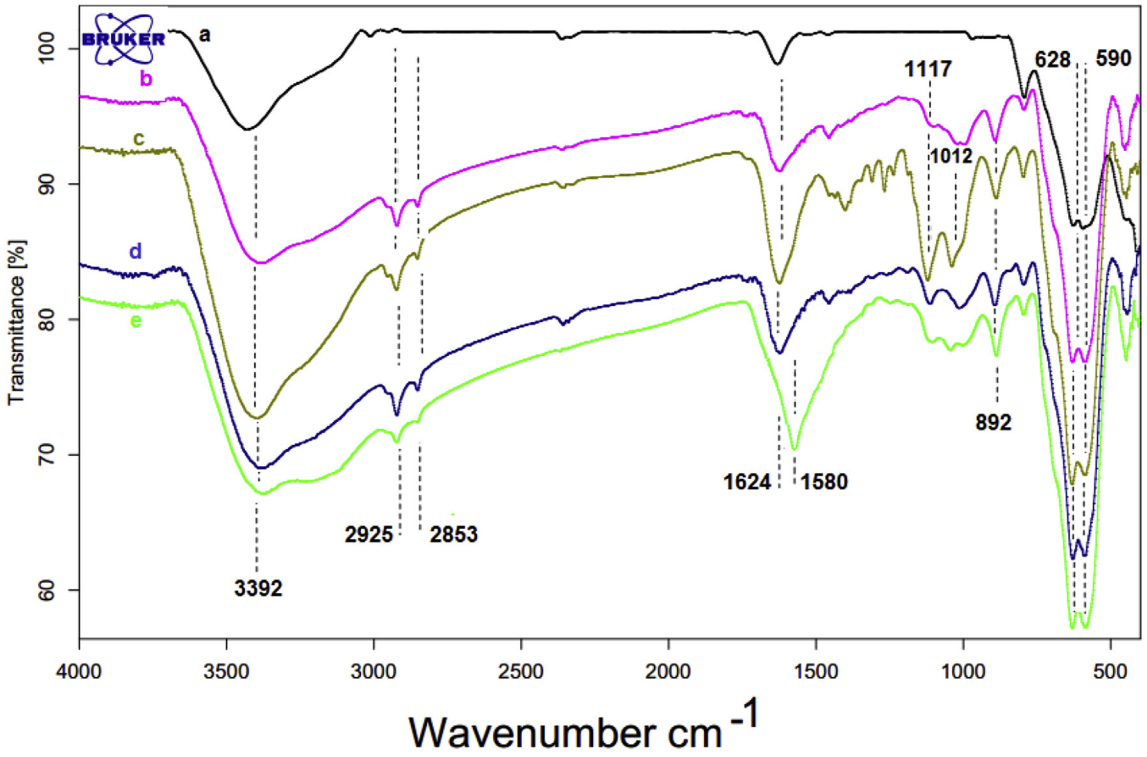

Fig. 2. FT-IR spectra of bare Fe_3O_4MNPs (a), CPTMS@Fe_3O_4MNPs(b), DETA-PTMS@Fe_3O_4MNPs(c), DAM-DETA-PTMS@Fe_3O_4MNPs (d) and Pd-Schiff-Base@Fe_3O_4MNPs (e).

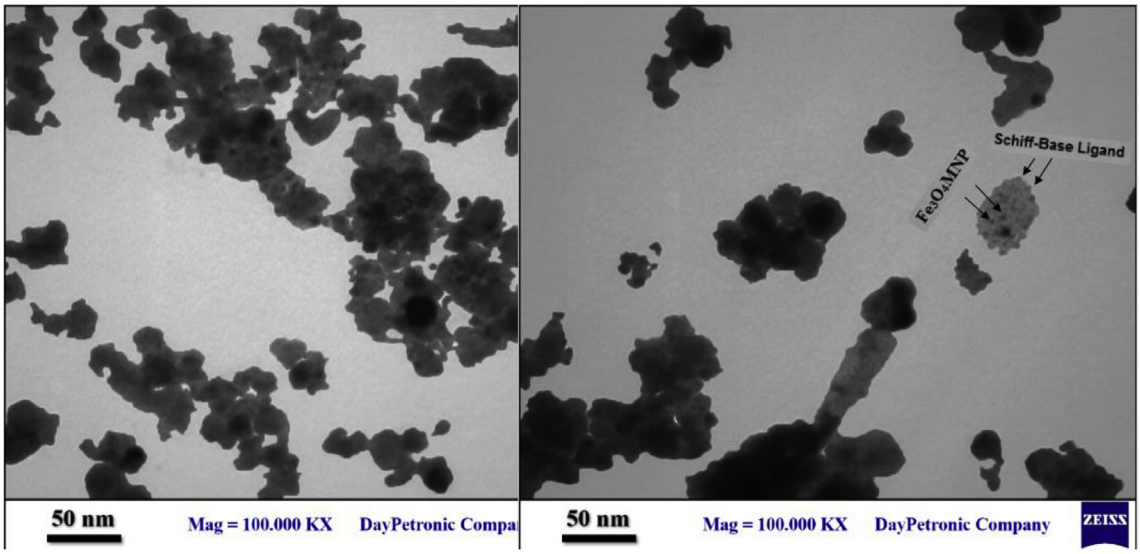

Fig. 3. TEM images of Pd-Schiff-Base@Fe_3O_4MNPs

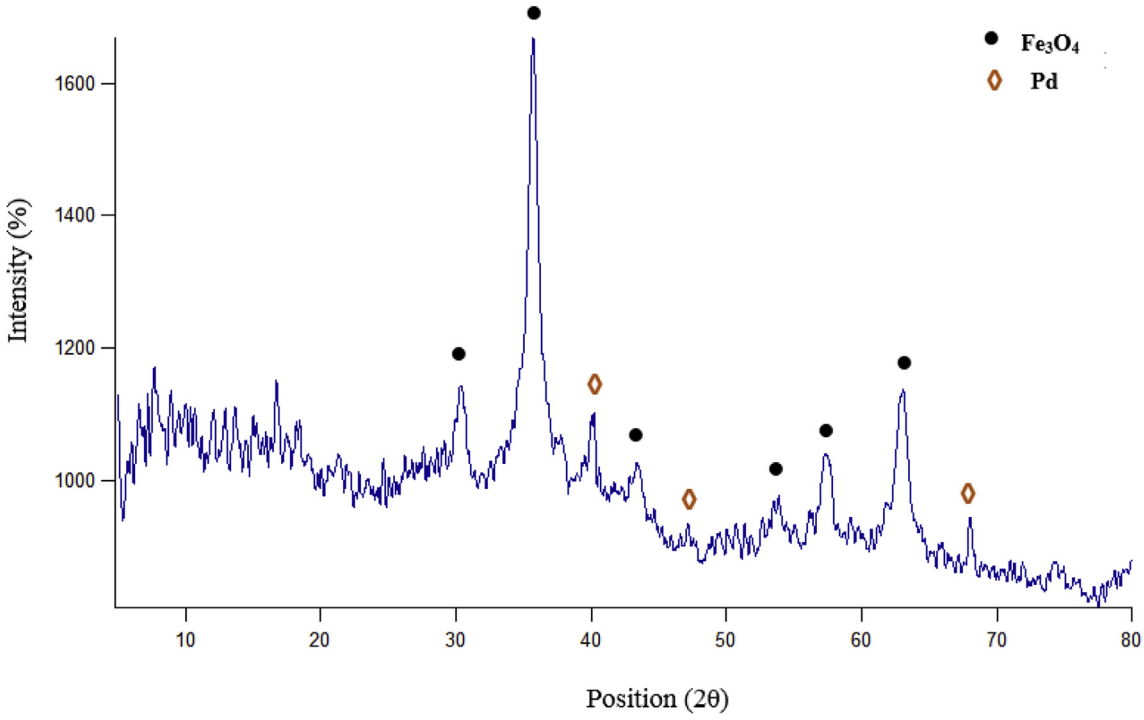

Fig. 4. XRD pattern of Pd-Schiff-Base@Fe_3O_4MNPs

preparation of Pd-Schiff-Base@Fe_3O_4MNPs, 210 mg of $PdCl_2$ dissolved in 70 mL of pure acetone and refluxed with the complex prepared at before step (DAM-DETA-PTMS@Fe_3O_4) in ethanol for overnight under nitrogen atmosphere. The Schiff-Base complex of palladium was separated by external magnet and dried under vacuum at 60 °C.

2.4. General procedure for synthesis of 5-substituted 1H-tetrazoles

A mixture of halobenzene (1 mmol), Na_3PO_4 (3 mmol), $K_2[Ni(CN)_4]$ (120.5 mg, 0.5 mmol), NaN_3 (3 mmol), DMF (2 mL) and Pd-Schiff-Base@Fe_3O_4MNPs (8 mg) was taken in 5 mL round bottomed flask and heated at 110 °C. After completion of reaction (monitored by TLC), the catalyst was separated from reaction mixture by an external magnet. The solvent was removed under reduced pressure and residue was dissolved in water (5 mL) and acidified with HCl, then a white solid was obtained.

2.5. General procedure for synthesis of benzamide

A mixture of halobenzene (1 mmol), Na_3PO_4 (3 mmol), $K_2[Ni(CN)_4]$ (120.5 mg, 0.5 mmol), DMSO (1.4 mL), H_2O (0.6 mL) and Pd-Schiff-Base@Fe_3O_4MNPs (5 mg) was taken in 5 mL round bottomed flask and heated at 100 °C. After completion of reaction

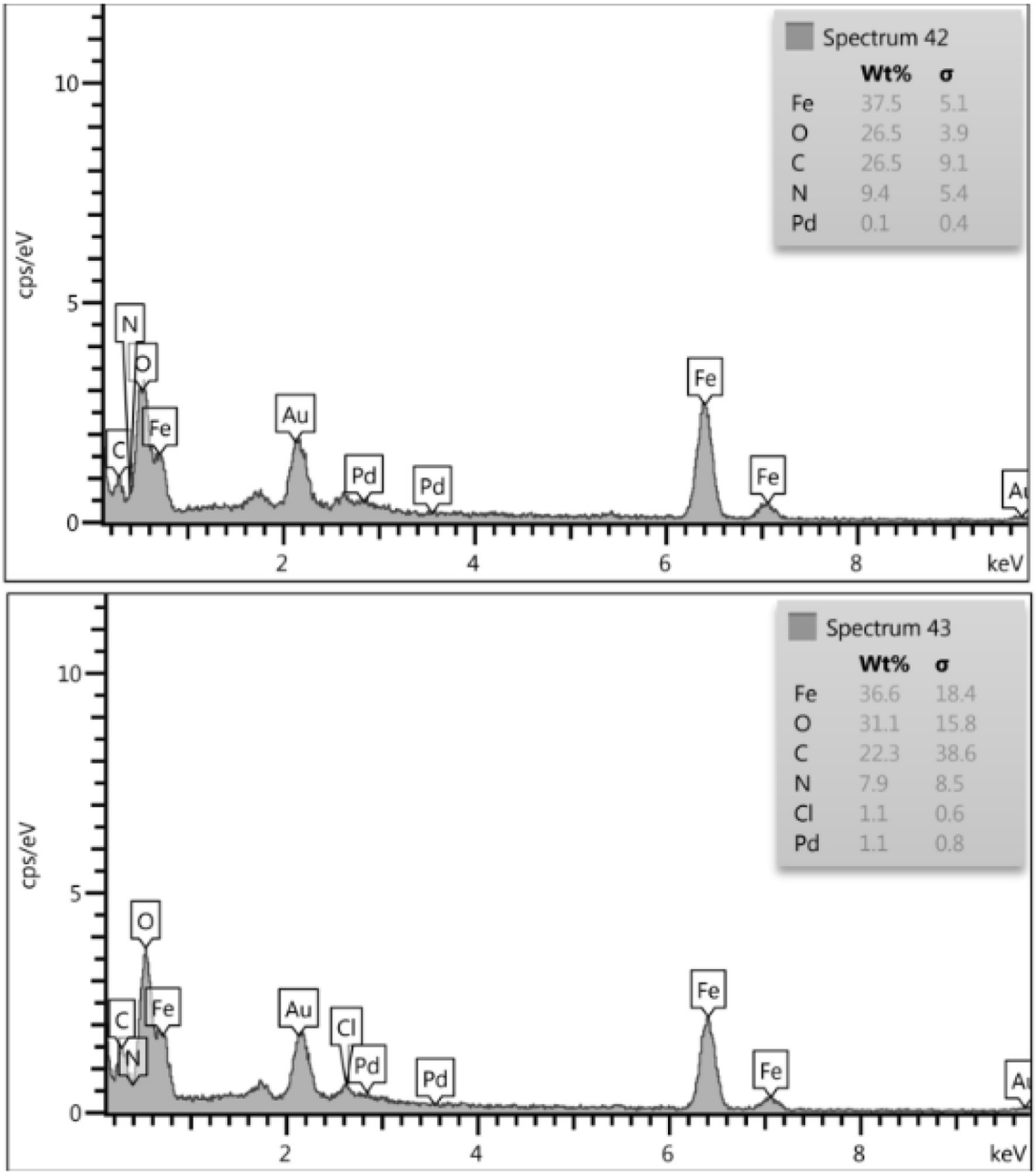

Fig. 5. EDX spectra of Pd-Schiff-Base@Fe_3O_4MNPs

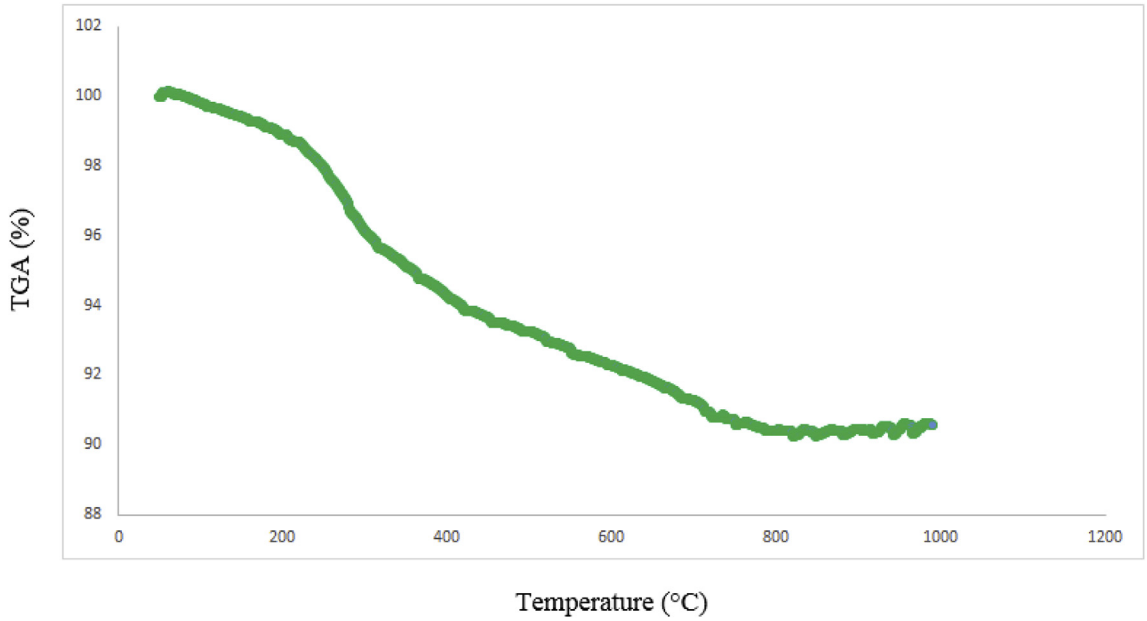

Fig. 6. TGA curve of Pd-Schiff-Base@Fe_3O_4MNPs

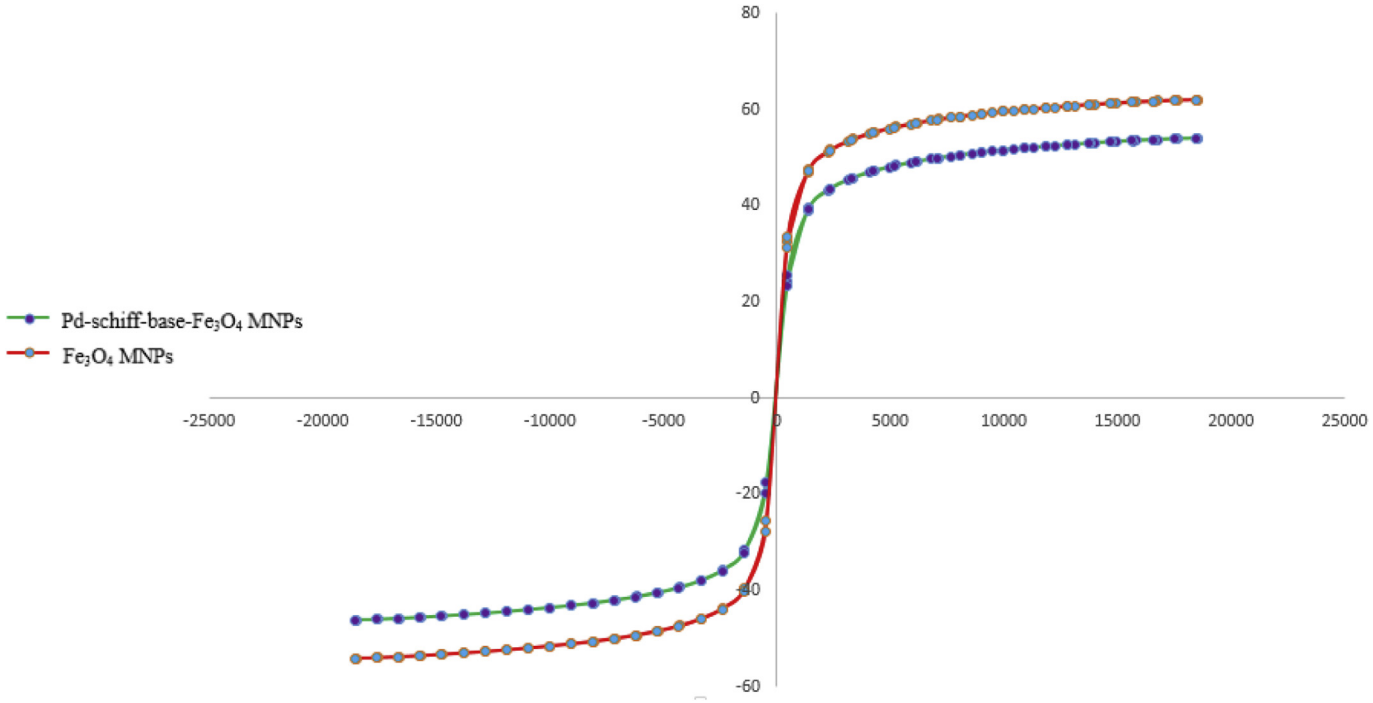

Fig. 7. Magnetization curves for Fe_3O_4MNPs and Pd-Schiff-Base@Fe_3O_4MNPs

(monitored by TLC), the catalyst was separated from reaction mixture by an external magnet. After evaporation of the solvent, the crude product was recrystallized in EtOH to gives pure Benzamide.

2.6. Physical and spectroscopic data for selected of 5-substituted 1H-tetrazole derivatives

2.6.1. 5-Phenyl-1H-tetrazole (3a)

FT-IR (KBr); ν_{max} (cm^{-1}) = 3467, 3083, 3046, 2981, 2918, 2848, 2768, 2698, 2612, 2577, 2475, 1890, 1614, 1570, 1505, 1434, 1404, 1285, 1258, 1187, 1164, 1125, 1086, 1054, 1027, 991, 823, 744, 711, 698, 615, 506, 486, 475, 457, 440, 420.^{1}H NMR (500 MHz, DMSO-d_6): δ (ppm) = 7.61 (d, 3H, J = 7 Hz, ArH), 8.10 (m, 2H, J = 7 Hz, ArH) ^{13}C NMR (125 MHz, DMSO-d_6): δ (ppm) = 124.9, 127.8, 130.3, 132.1, 156.1.

2.6.2. 5-(3-Nitrophenyl)-1H-tetrazole (3c)

FT-IR (KBr); ν_{max} (cm^{-1}) = 3101, 3079, 2998, 2909, 2862, 2695, 2608, 2483, 1988, 1931, 1796, 1754, 1627, 1588, 1531, 1479, 1409,

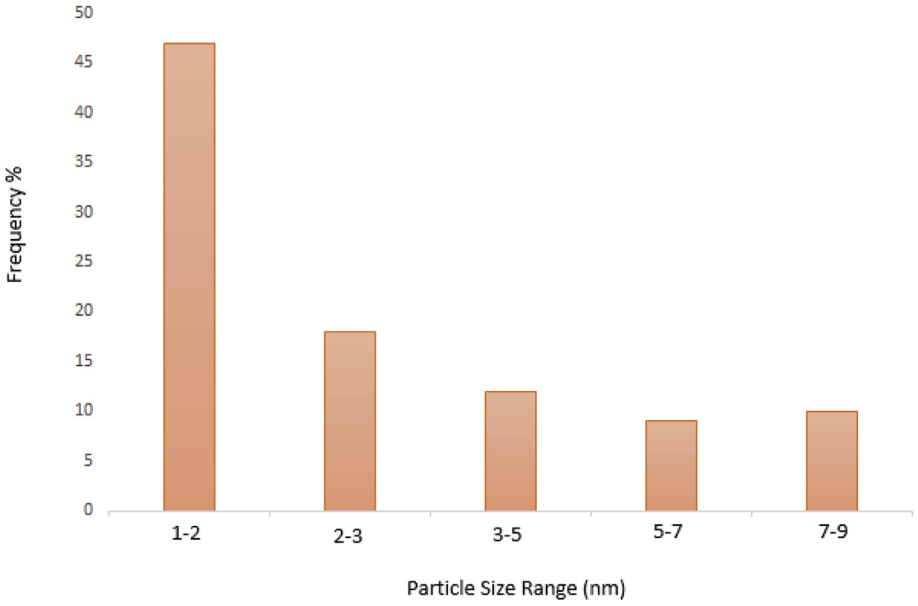

Fig. 8. Particle range size of Pd-Schiff-Base@Fe_3O_4MNPs

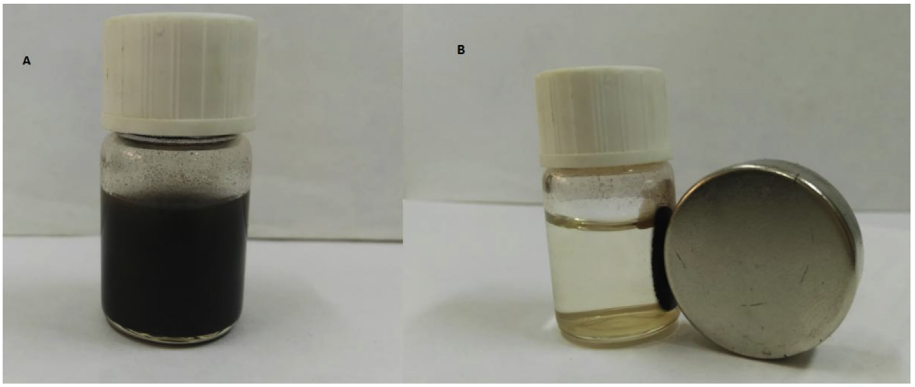

Fig. 9. Photograph of the aqueous solution A, with dispersed Pd-Schiff-Base@Fe_3O_4MNPs and B after 5 s applied magnetic field.

1348, 1307, 1278, 1251,1176, 1163, 1090, 1059, 1033, 992, 916, 870, 817, 765, 738, 726, 709, 677, 655, 551, 523, 445, 424 ^{1}H NMR (500 MHz, DMSO-d_6): δ (ppm) = 7.79 (t, 1H, J = 8 Hz, ArH), 8.42 (d, 1H, J = 8 Hz, ArH), 8.59 (d, 1H, J = 8 Hz, ArH), 8.10 (s, 1H, ArH) ^{13}C NMR (125 MHz, DMSO-d_6): δ (ppm) = 122.2, 126.3, 126.9, 131.9, 133.8, 149.0, 157.7.

2.6.3. 2-(1H-tetrazol-5-yl) phenol (3f)

FT-IR (KBr); ν_{max} (cm^{-1}) = 3096, 1597, 1526, 1472, 1449, 1375, 1344, 1287, 1255, 1233, 1205, 1160, 1143, 1096, 1059, 987, 911, 829, 762, 743, 716, 695, 668, 526, 466.^{1}H NMR (500 MHz, DMSO-d_6): δ (ppm) = 7.13 (t, 1H, J = 7.5 Hz, ArH), 7.2 (d, 1H, J = 7.5 Hz, ArH), 7.33 (d, 1H, J = 7.5 Hz, ArH), 7.51 (t, 1H, J = 7.5 Hz, ArH), 7.92 (s, 1H, OH) ^{13}C NMR (125 MHz, DMSO-d_6): δ (ppm) = 111.4, 117.2, 120.6, 129.9, 133.5, 152.7, 156.2.

2.7. Physical and spectroscopic data for benzamide

FT-IR (KBr); v max (cm^{-1}) = 3293, 3216, 3085, 2966, 1698, 1617, 1529, 1484, 1381, 1342, 1308, 1283, 1235, 1217, 1172, 1145, 1106, 1071, 1033, 1001, 975, 756, 535.^{1}H NMR (400 MHz, DMSO- d_6): δ (ppm) = 5.91 (bs, 2H, NH_2), 7.44–7.58 (m, 3H, ArH), 7.8–7.84 (m, 2H, ArH). ^{13}C NMR (100 MHz, DMSO- d_6): δ (ppm) = 127.3, 128.5, 132, 133.5, 169.5.

3. Result and discussion

The morphology of the Pd-Schiff-Base@Fe_3O_4MNPs was studied by scanning electron microscopy (SEM) (Fig. 1). The SEM image shows the average size of particles, roughly 25 nm.

FT-IR spectra of bare Fe_3O_4MNPs, CPTMS@Fe_3O_4MNPs, DETA-PTMS@Fe_3O_4MNPs, DAM-DETA-PTMS@Fe_3O_4MNPs and Pd-Schiff-Base@Fe_3O_4MNPs are shown in Fig. 2. The FT-IR spectrum of Fe_3O_4MNPs (2a) is exhibits characteristics peaks at 590 and 628 cm^{-1} corresponding to Fe–O band in tetrahedral sites of bare magnetic nanoparticles [56] and the broad band at 3392 cm^{-1} which is assigned to asymmetric and symmetric stretching vibrations of –OH band of surface of magnetic nanoparticles. Also a peak appear at 1624 cm^{-1} is assigned to the bending vibration of OH band or stretching vibrational mode of an adsorbed water layer [57]. In the FT-IR spectrum of CPTMS@Fe_3O_4MNPs (2b), the presence of the anchored Cl-propyl group is confirmed by C–H

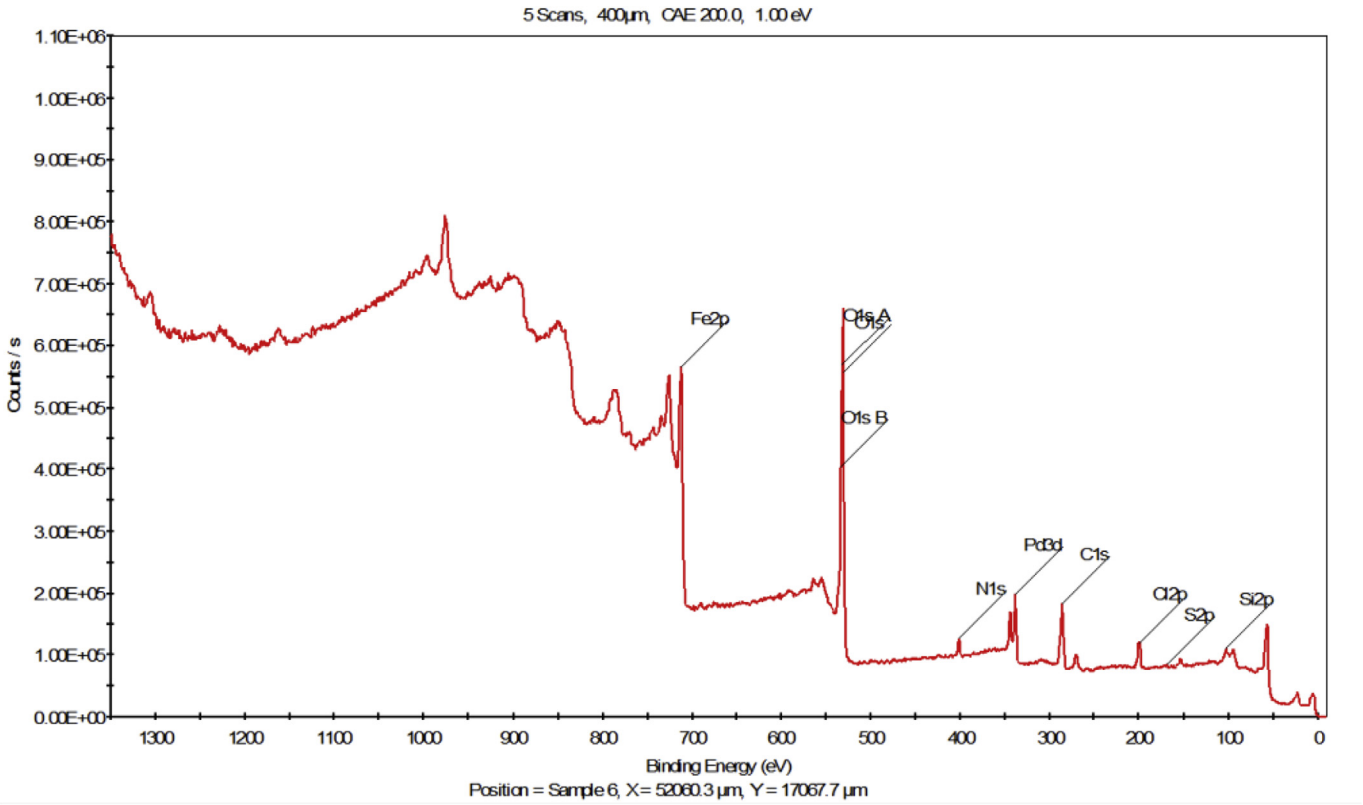

Fig. 10. Full XPS spectrum of Pd-Schiff-Base@Fe_3O_4MNPs

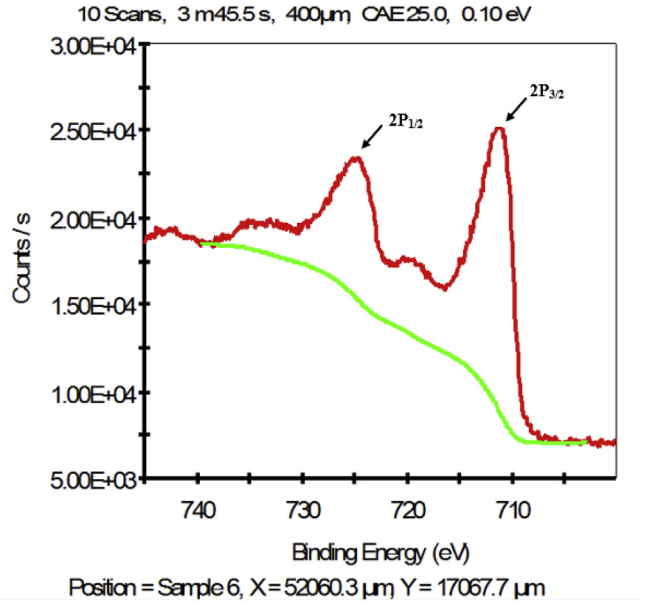

Fig. 11. XPS spectrum of Fe 2P of Pd-Schiff-Base@Fe_3O_4MNPs

stretching vibrations that appear at 2853 and 2925 cm^{-1}, the peak at 892 cm^{-1} which is attributed to Fe–O–Si stretching vibration. The existence of the characteristic C–N stretching at 1012 and1117 cm^{-1}on DETA-PTMS@Fe_3O_4MNPS (2c), are evidences to confirm the formation of desired ligand [58]. A peak at 1624 cm^{-1} in the spectrum of DAM-DETA-PTMS@Fe_3O_4MNPs (2d), is due to C=N bond formation.

In the spectrum of Pd-Schiff-Base@Fe_3O_4MNPs (2e), C=N bond absorption shift to lower frequency, 1580 cm^{-1}, in comparing of C=N bond absorption in spectrum of DAM-DETA-PTMS@Fe_3O_4MNPs (2d) and it's due to successful bond formation between palladium and C=N bonds.

TEM micrographs of synthesized catalyst (Pd-Schiff-Base@-Fe_3O_4MNPs) are given in Fig. 3. Generally, nanoparticles have spherical morphology and their sizes are varying ranges and summarized in Fig. 8.

In order to formation of crystal phase in Pd-Schiff-Base@-Fe_3O_4MNPs X-Ray Diffraction pattern (XRD) was performed (Fig. 4). As shown in Fig. 4, the iron oxide phase was identified by peak positions at 30.3° (220), 35.67° (311), 43.39° (400), 53.66° (422), 57.34° (511) and 62.93° (440) agreement with the standard magnetite XRD pattern [59] and also peaks at 40.21°, 47.15° and 68.01°confirm the presence of palladium specie [60,61].

The EDX spectra of Pd-Schiff-Base@Fe_3O_4MNPs are shown in Fig. 5. EDX spectra at different points of the images confirm the presence of Pd in the catalyst and it is attribute atomic absorption spectroscopy. Fig. 5, confirms the presence of C, N, O, Fe, Cl and Pd species. Also for more studied, we have determined the exact amount of palladium on catalyst support by ICP–AES (Inductively Coupled Plasma-Atomic Emission Spectroscopy) technique. The palladium amount of immobilized catalyst on Pd-Schiff-Base@-Fe_3O_4MNPs was found 1.92×10^{-3} mol g^{-1}.

TGA is an efficient and fascinating technique to investigate the thermal stability of immobilized catalyst relative to that of magnetic nanoparticles. Also the bond formation between magnetite nanoparticles and catalyst can be as well interpreted and verified by TGA. The TGA curve of the Pd-Schiff-Base@Fe_3O_4MNPs shows the mass loss of the organic functional groups as it decomposes upon heating. As shown in Fig. 6 the TGA curve of the Pd-Schiff-

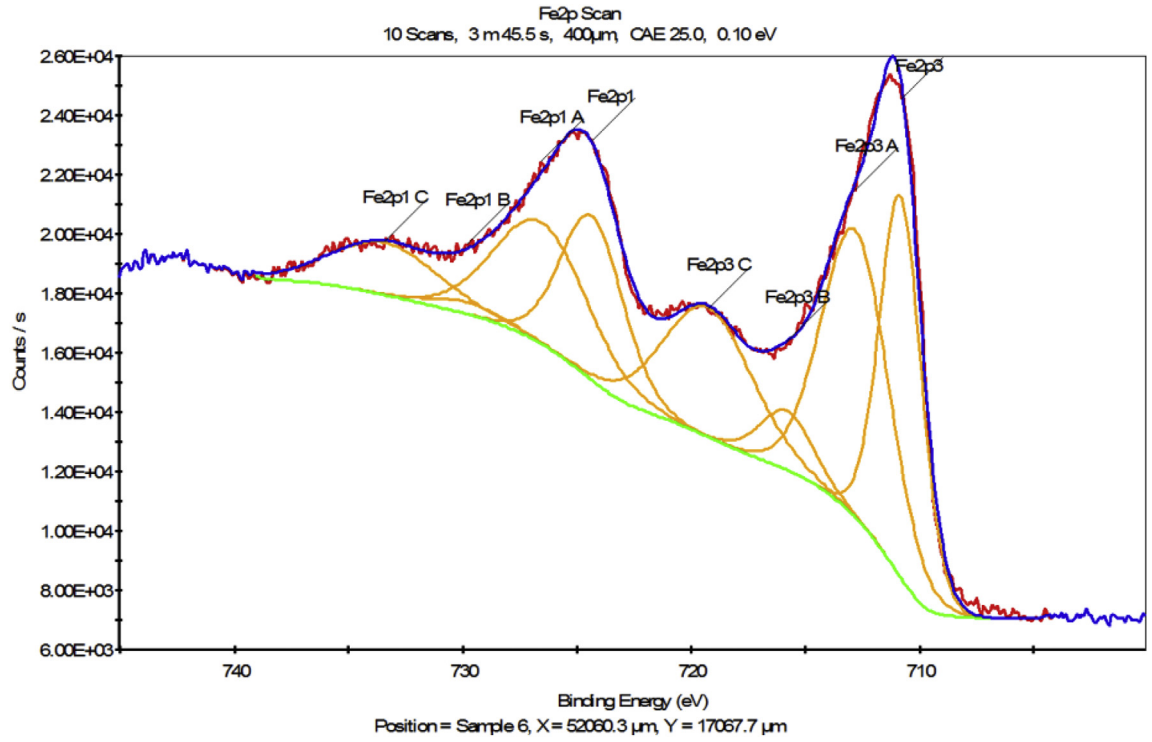

Fig. 12. Deconvoluted XPS spectrum of Fe 2P of Pd-Schiff-Base@Fe_3O_4MNPs

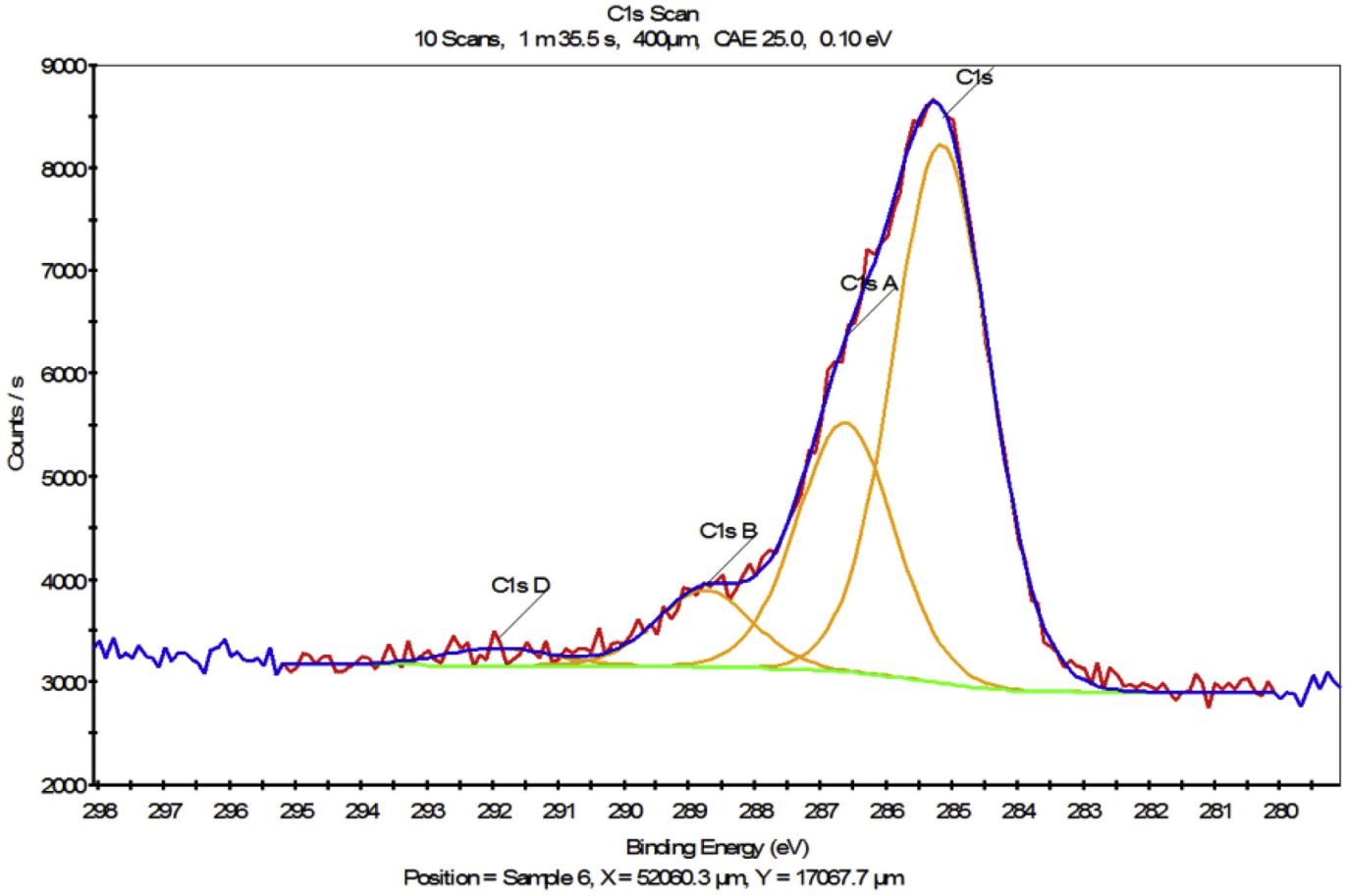

Fig. 13. XPS spectrum of C 1S of Pd-Schiff-Base@Fe_3O_4MNPs

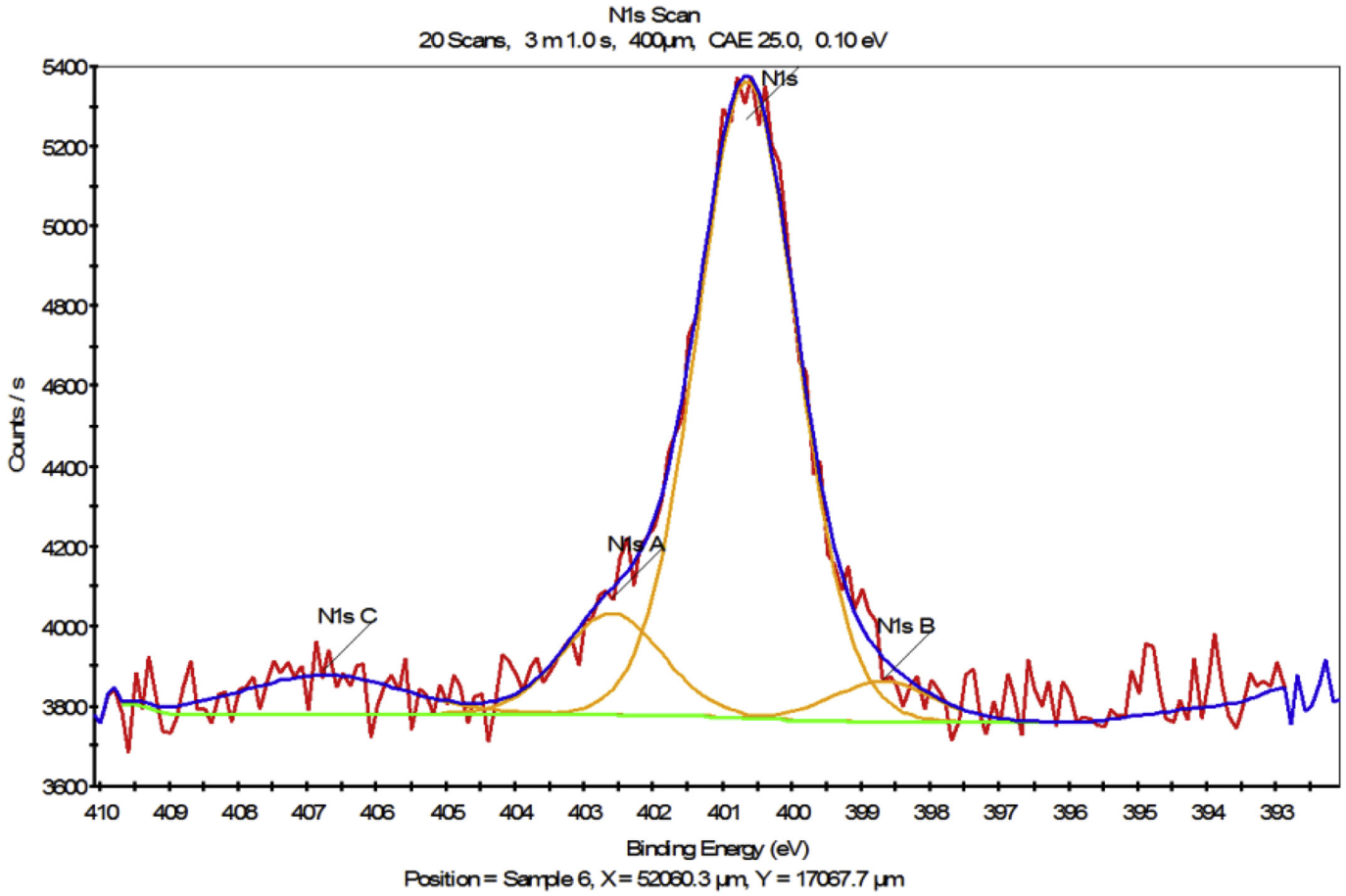

Fig. 14. XPS spectrum of N 1S of Pd-Schiff-Base@Fe_3O_4MNPs

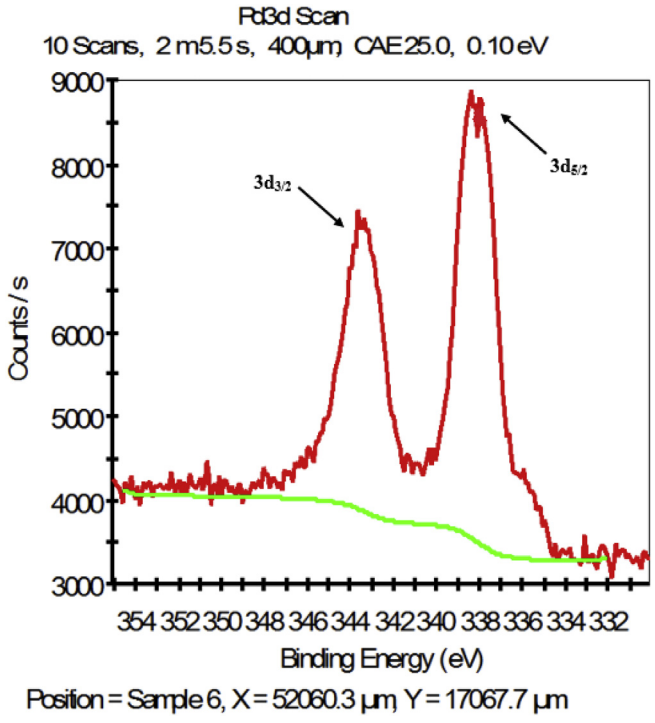

Fig. 15. XPS spectrum of Pd 3d of Pd-Schiff-Base@Fe_3O_4MNPs

Base@Fe_3O_4MNPs shows small amount of weight loss blow 250 °C is due to desorption of physically adsorbed solvents and surface hydroxyl groups. Furthermore a weight loss about of 5% from 250 to 700 °C, resulting from the decomposition of immobilized organic spaces on Fe_3O_4MNPs surface.

Superparamagnetic particles are beneficial for magnetic separation, the magnetic property of Fe_3O_4MNPs and Pd-Schiff-Base@-Fe_3O_4MNPs were characterized by VSM. As shown in Fig. 7, VSM measurement for Fe_3O_4MNPs shows the saturation magnetization (M_s) is 62.10 emu g^{-1}, while M_s of Pd-Schiff-Base@Fe_3O_4MNPs is decreased to 54.04 due to the anchored palladium complex.

The magnetic separation ability is further studied in reaction media through a separation process by placing an external magnet near the reaction mixture vessel. The Pd-Schiff-Base@Fe_3O_4MNPs were attracted towards the external magnet in 5 s (Fig. 9).

Figs. 10–15 show the XPS elemental survey scans of Pd-Schiff-Base@Fe_3O_4MNPs. As shown in Fig. 10, the peaks corresponding to palladium, carbon, nitrogen, chlorine oxygen, iron and silicon clearly observed.

Fig. 11, displays the iron binding energy of Pd-Schiff-Base@-Fe_3O_4MNPs. This spectrum exhibits two major peaks centered at 711 and 724.3 eV, which are assigned to Fe $2P_{3/2}$ and Fe $2P_{1/2}$ for Fe_3O_4, respectively [62–65]. Also a satellite peak at 719.8 eV is corresponding to Fe^{3+} ions in γ-Fe_3O_4 [66]. It may be due to partial oxidation of Fe_3O_4MNPs.

In order to determine the Fe^{3+}/Fe^{2+} ratio, deconvolution of Fe $2P_{1/2}$ and Fe $2P_{3/2}$ peaks accomplished (Fig. 12). The Fe^{3+}/Fe^{2+} ratio equaled 1.8 based area under curves [67]. This value is acceptable in

Table 1
BET results of Fe_3O_4MNPs and Pd-Schiff-Base@Fe_3O_4MNPs

Sample	BET surface area (m^2g^{-1})	Pore diameter (BJH) (nm)	Pore volume (cm^3/g)
Fe_3O_4MNPs	178.2	1.72	0.3
Pd-Schiff-Base@Fe_3O_4MNPs	149.1	1.17	0.22

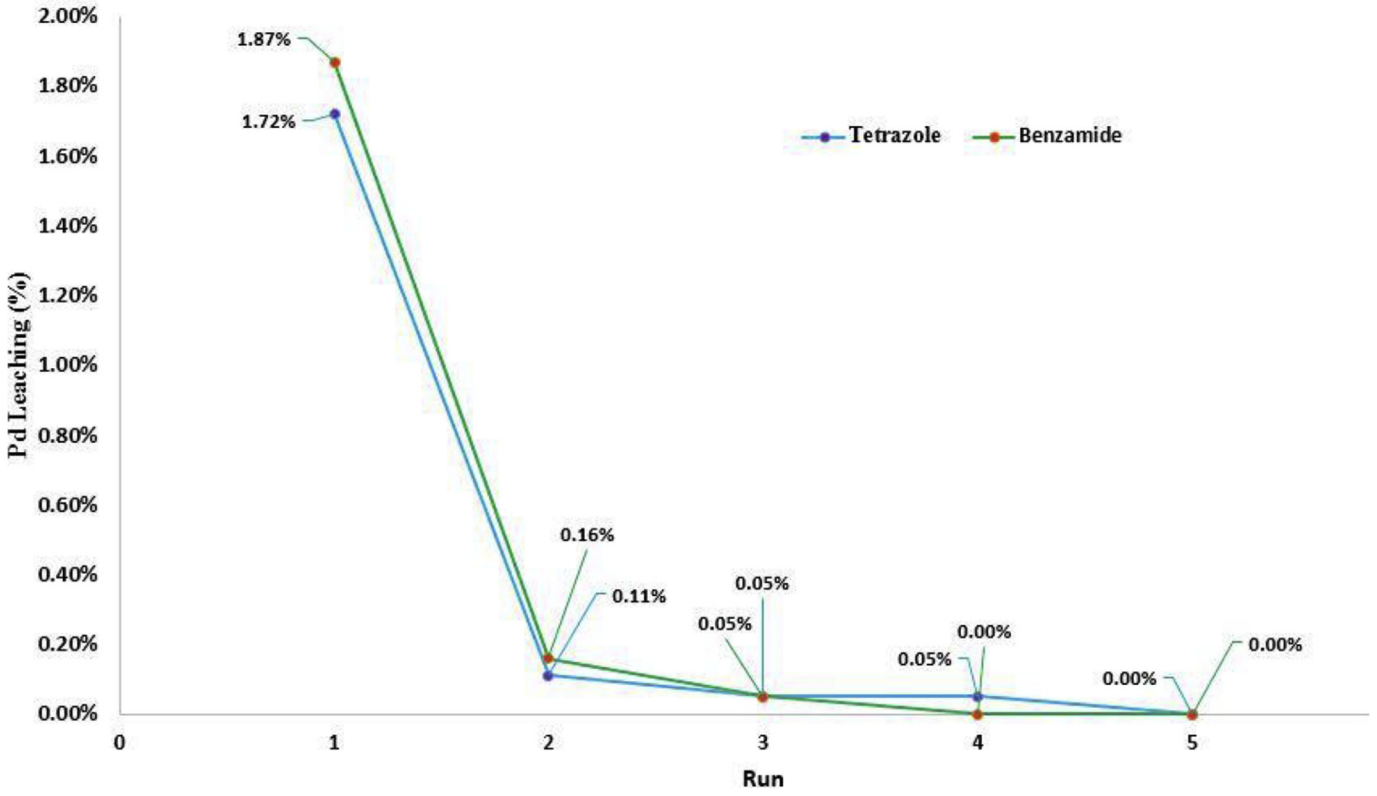

Fig. 16. Palladium leaching percent of Pd-Schiff-Base@Fe_3O_4MNPs

Table 2
Palladium leaching study of Pd-Schiff-Base@Fe_3O_4MNPs

Cycle	Residue Palladium (mmol/g)		Palladium Leaching (%)	
_	Tetrazole	Benzamide	Tetrazole	Benzamide
1	1.887	1.884	1.72	1.87
2	1.885	1.881	0.11	0.16
3	1.884	1.880	0.05	0.05
4	1.883	1.880	0.05	0.00
5	1.883	1.880	0.00	0.00

comparison with experimental part.

In order to study of types of carbon covalent bonds, deconvolution of C 1s accomplished. As shown in Fig. 13, three peaks at 285, 286.7 and 288.9 eV are corresponding carbon-carbon single bond (C–C), carbon-nitrogen double bond (C=N) and carbon-nitrogen single bond (C–N), respectively [68–70]. Also, as shown in Fig. 14, the peaks at 389.5.400.6 and 403 eV reflect the bonding structure of carbon-nitrogen double bond (C=N), carbon-nitrogen single bond (C–N) and nitrogen-oxygen single bond (N–O), respectively [70,71].

Fig. 15, shows the palladium binding energy of Pd-Schiff-Base@Fe_3O_4MNPs. This spectrum exhibits two prominent peaks at 338.3 and 343.5 eV, readily assigned to Pd $3d_{3/2}$ and Pd $3d_{3/2}$, respectively [72,73].

In order to propose the structure of catalyst, we evaluated information from experimental section and characterization data. The proposed catalyst structure summarized in Scheme 2.

Some textural and physicochemical properties of synthesized samples including pore diameter (DBJH), the BET surface area and pore volume are given in Table 1. As seen, an obvious decrease in BET surface area, pore volume and pore diameter was detected after the modification which confirmed the ligand grafting on Fe_3O_4MNPs surface.

Metal leaching and heterogeneity of the catalyst, Pd-Schiff-Base@Fe_3O_4MNPs, was studied by hot filtration test and ICP analysis. Palladium leaching of the catalyst was determined as following procedure. We considered model reaction condition without reagents as a new condition. A mixture of catalyst (Pd-Schiff-Base@Fe_3O_4MNPs), solvent (DMF or DMSO + H_2O) and additive was taken in 5 mL round bottomed flask and sated optimized conditions. After completion of the reaction (optimized time for model reaction), the catalyst was separated by an external magnet and washed with hot EtOH, then dried in an oven at 120 °C for 2 h. The amount of palladium in solution determined by ICP-AES. This experiment was determined for five time recycled. Above procedure performed for the synthesis of 5-phenyl-1*H*-tetrazole and Benzamide and data summarized in Fig. 16 and Table 2. These results indicate that Pd leaching of the catalyst was negligible. Further, heterogeneity of the catalyst was confirmed by hot

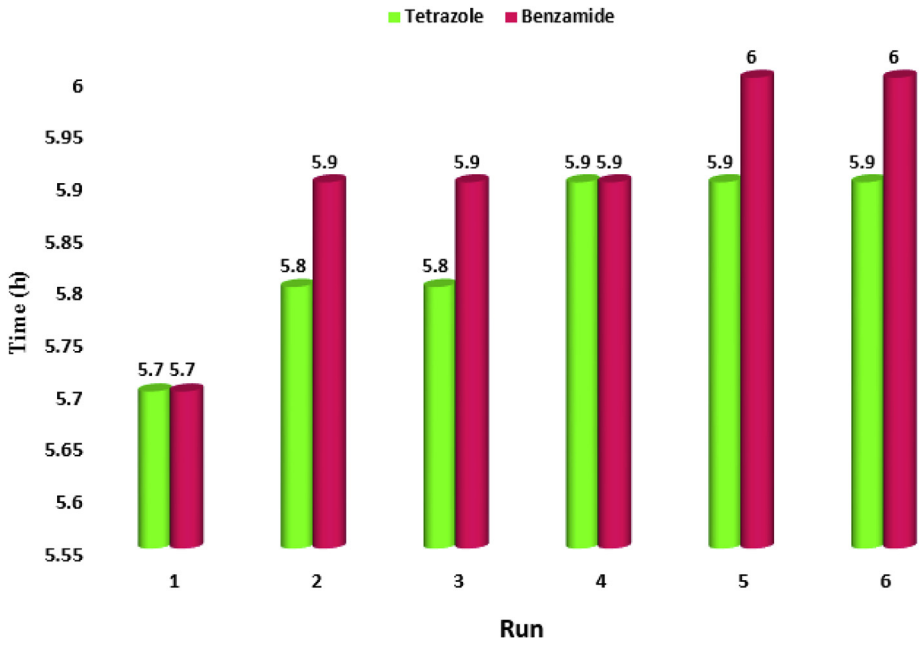

Fig. 17. Reusability of Pd-Schiff-Base@Fe_3O_4MNPs

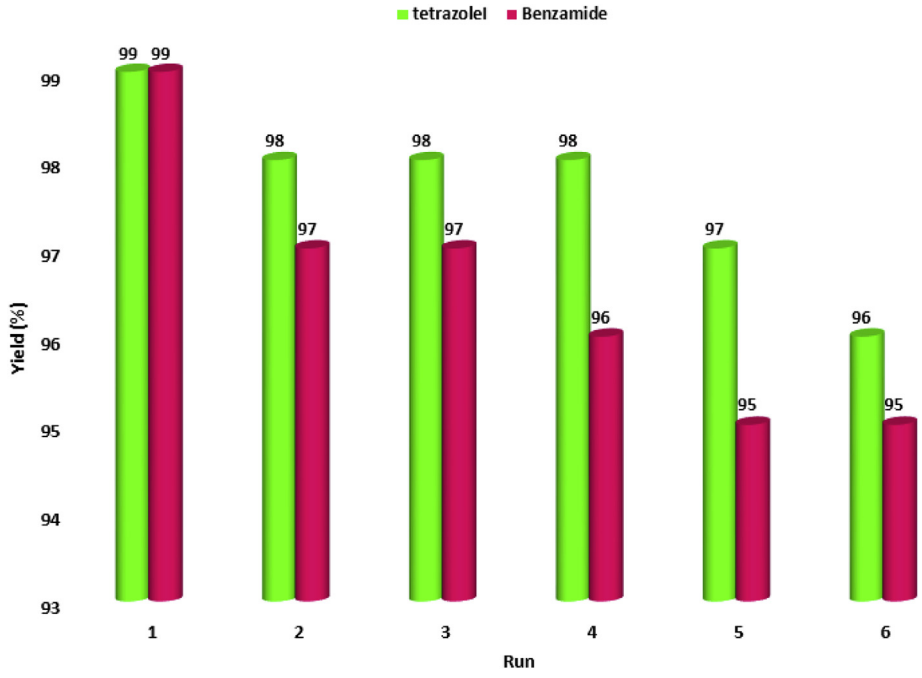

Fig. 18. Reusability of Pd-Schiff-Base@Fe_3O_4MNPs

filtration test the synthesis of for 5-substituted 1*H* -tetrazole (T in Scheme 1) and Benzamide (B in Scheme 1). In this study we found the yield of products in the half time of the reaction was 56% and 50% for T and B, respectively. Then the reaction was repeated and in the half of the reaction, the catalyst was recovered and allowed the filtrate to react further. The yield of reactions in this stage was 58% and 53% for T and B, respectively that confirmed the leaching of palladium has not been occurred.

For reusability study of Pd-Schiff-Base@Fe_3O_4 MNPs, as magnetically nanocatalyst can be easily recovered from the reaction mixture and used for synthesis of 5-substituted 1*H*-tetrazoles and Benzamide. To investigate this issue, the recyclability of catalyst was examined for the synthesis of 3a and Benzamide under optimized reaction conditions. The catalyst was separated from reaction mixture using an external magnet and reused six times with negligible loss of activity. Partial loss of activity may be due to leaching of palladium from the catalyst (Figs. 17 and 18).

In order to optimize the reaction conditions, initially, the reaction of iodobenzene, trisodium phosphate, $K_2[Ni(CN)_4]$ and sodium azide was considered as model reaction. The reaction conditions and media have dramatic effects on the yield and time

Table 3
Optimization of reaction conditions for synthesis of 5-substituted 1*H*-tetrazole.

Entry	Solvent	Catalyst amount	Base (mmol)	Temp. (°C)	Time (h)	Yield (%)[a]
1	DMF	8	Na_3PO_4 (3)	90	12	78
2	DMF	8	Na_3PO_4 (3)	100	7.5	92
3	DMF	8	Na_3PO_4 (3)	110	5.7	99
4	DMF	8	Na_3PO_4 (3)	120	6	70
5	DMF	7	Na_3PO_4 (3)	110	10.1	89
6	DMF	9	Na_3PO_4 (3)	110	5.7	96
7	DMF	10	Na_3PO_4 (3)	110	7.3	90
8	DMF	8	Et_3N (3)	110	8	91
9	DMF	8	NaOH (3)	110	10	65
10	DMF	8	KOH (3)	110	10	79
11	DMF	8	K_2CO_3 (3)	110	5.8	98
12	DMF	8	Na_3PO_4 (2)	110	8.5	89
13	DMSO	8	Na_3PO_4 (3)	110	N.R.[b]	–
14	EtOH	8	Na_3PO_4 (3)	Reflux	48	71
15	H_2O	8	Na_3PO_4 (3)	Reflux	N.R.[b]	–
16	DMF	8[c]	Na_3PO_4 (3)	110	N.R.[b]	–
17	DMF	–	Na_3PO_4 (3)	110	N.R.[b]	–

The scope and generality of this type of reaction is illustrated with respect to the different arylhalides, $K_2[Ni(CN)_4]$, trisodium phosphate and sodium azide. The results summarized in Table 4.

[a] Yield refer to isolated pure product.
[b] The reactions stop after 72 h
[c] The catalyst used is Fe_3O_4MNP.

Table 4
Synthesis of 5-substituted 1*H*-tetrazoles catalyzed by Pd-Schiff-Base@Fe_3O_4MNPs

Entry	Substrate	Product	Time (h)	Yield[a] (%)	Found	M.p. (C) Reported [ref]
3a		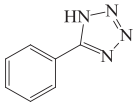	5.7	99	214–215	212-214 [74]
3b		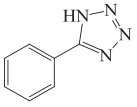	9	86	214–215	212-214 [74]
3c	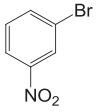	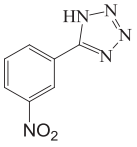	7.8	95	145–146	145-146 [75]
3d	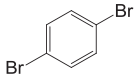	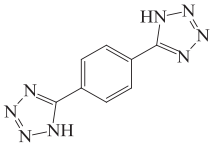	13.1	88	245–248	Not found
3e	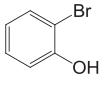	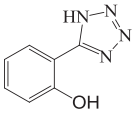	14.3	65	223–225	221-224 [76]
3f	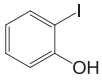	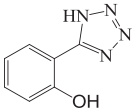	5.9	99	223–225	221-224 [76]
3 g	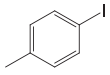	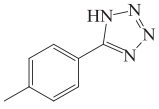	10.9	81	241–243	242-245 [74]

[a] Yield refer to isolated pure product.

Table 5
One pot cascade reaction, for the synthesis of Benzamide from iodobenzene, $K_2[Ni(CN)_4]$ and trisodium phosphate catalyzed by Pd-Schiff-Base@Fe_3O_4MNPs.

Entry	Solvent	Catalyst (mg)	Base (mmol)	Temp. (°C)	Time (h)	Yield (%)[a]
1	DMSO + H_2O (3:7)	Pd–S.B.[b] (5)	Na_3PO_4 (3)	100	16	68
2	DMSO + H_2O (1:1)	Pd–S.B.[b] (5)	Na_3PO_4 (3)	100	7	89
3	DMSO + H_2O (7:3)	Pd–S.B.[b] (5)	Na_3PO_4 (3)	100	5.5	99
4	DMSO	Pd–S.B.[b] (5)	Na_3PO_4 (3)	100	N.R.[c]	–
5	H_2O	Pd–S.B.[b] (5)	Na_3PO_4 (3)	100	N.R.[c]	–
6	DMF	Pd–S.B.[b] (5)	Na_3PO_4 (3)	100	N.R.[c]	–
7	DMF + H_2O (7:3)	Pd–S.B.[b] (5)	Na_3PO_4 (3)	100	N.R.[c]	–
8	DMF + H_2O (1:1)	Pd–S.B.[b] (5)	Na_3PO_4 (3)	100	N.R.[c]	–
9	DMF + H_2O (7:3)	Pd–S.B.[b] (5)	Na_3PO_4 (3)	100	48	7
10	EtOH	Pd–S.B.[b] (5)	Na_3PO_4 (3)	100	N.R.[c]	–
11	DMSO + H_2O (7:3)	Pd–S.B.[b] (5)	Na_3PO_4 (3)	110	5.7	99
12	DMSO + H_2O (7:3)	Pd–S.B.[b] (5)	Na_3PO_4 (2)	90	6.6	97
13	DMSO + H_2O (7:3)	Pd–S.B.[b] (5)	Et_3N (3)	100	N.R.[c]	–
14	DMSO + H_2O (7:3)	Pd–S.B.[b] (5)	NaOH (3)	100	N.R.[c]	71
15	DMSO + H_2O (7:3)	Pd–S.B.[b] (5)	KOH (3)	100	N.R.[c]	–
16	DMSO + H_2O (7:3)	Pd–S.B.[b] (5)	K_2CO_3 (3)	100	48	20
17	DMSO + H_2O (7:3)	Pd–S.B.[b] (5)	Na_3PO_4 (2)	100	6.8	95
18	DMSO + H_2O (7:3)	Fe_3O_4[d](5)	Na_3PO_4 (3)	100	N.R.[c]	–
19	DMSO + H_2O (7:3)	$PdCl_2$ (1.7)	Na_3PO_4 (3)	100	5	71

[a] Yield refer to isolated pure product.
[b] Refers to Pd-Schiff-Base@Fe_3O_4MNPs
[c] The reactions stop after 72 h
[d] The used catalyst is Fe_3O_4MNP.

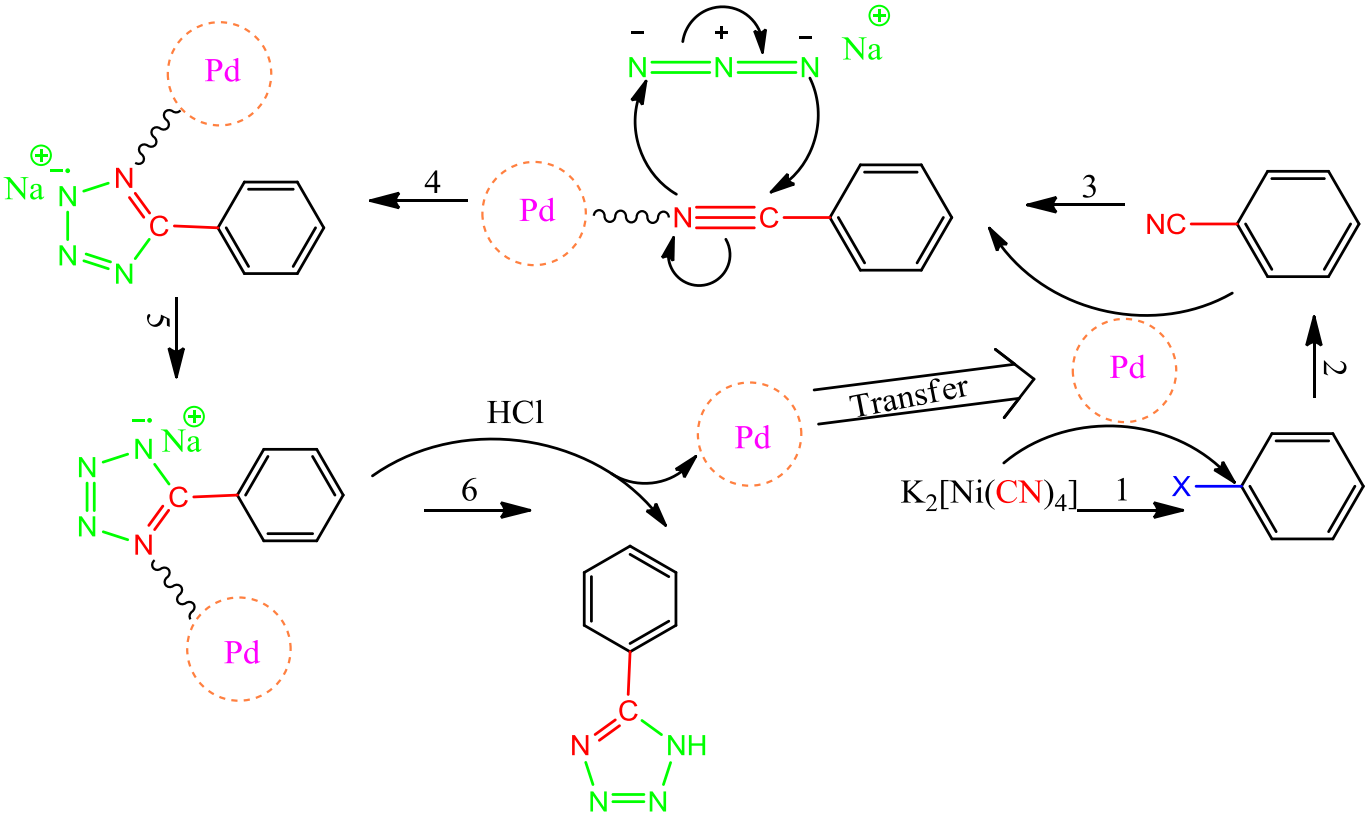

Scheme 3. Plausible mechanism for the synthesis of 5-substituted 1*H*-tetrazoles.

of reaction due to the hard reaction conditions for synthesis of tetrazoles. The model reaction was optimized for the various parameters such as temperature, solvent, catalyst amount and base. the result summarized in Table 3. In the preliminary stage of this investigation, the synthesis of 5-substituted 1*H*-tetrazole was performed at various temperatures (Table 2, Entries1-4). The best result was obtained at 110 °C. The catalytic performance of Pd-Schiff-Base@Fe_3O_4MNPs was investigate in the model reaction with different amount of catalyst (Table 2, Entries3, 5–7). As shown in Table 3, at a lower catalyst amount (7 mg), an 89% yield of compound 4a was observed after 10.1 h (Table 3, entry 5). On increasing the catalyst weight to 8 mg, the yield compound 4a increased up to 99% after 5.7 h (Table 3, entry 3). The increase in the product yield with an increase in the catalyst weight can be

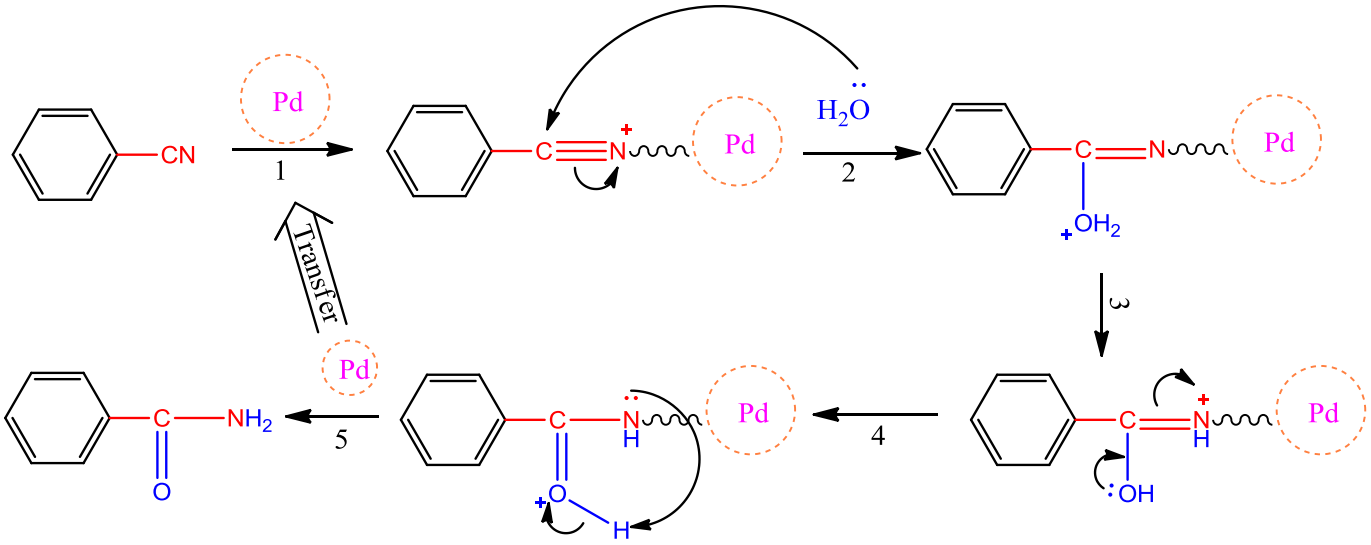

Scheme 4. Plausible mechanism for the synthesis of benzamide.

attributed to an increase in the availability of catalytically active sites required for this reaction. On further increasing the amount of catalyst, namely, amounts greater than 8 mg, any appreciable change or improvement was not observed in product yield after complete the reaction (Table 3, entries 6,7). The collect results in Table 3 clearly demonstrate that the reaction rate and product yield not only depended strongly on the amount of catalyst (Table 3, entries 3, 5–8), but also that the presence of catalyst is a pivotal topic in this process because it was found that once the reaction was carried out in the absence of catalyst (Table 3, entry 17), any yield of the desired product was not observed after 72 h. In order to find out the best base for tetrazole reaction the model reaction was performed in presence of various bases (Table 3, entries 4, 8–11). The results show trisodium phosphate is very effective for this conditions. Also the effects of various solvents on the model reaction were studied by using EtOH, H_2O and DMSO instead of DMF (Table 3, entries 13–15). The results show that the DMF was more effective than other solvents.

Table 5 shows the result of one pot synthesis of Benzamide in various conditions. The data show that only pathway for the synthesis of the benzamide is the reaction of between arylhalide, $K_2[Ni(CN)_4]$, trisodium phosphate and (DMSO + H_2O). Other solvents, bases and catalysts are not efficient in the synthesis of benzamide.

A plausible mechanism for the synthesis of 5-substituted 1*H*-tetrazoles and benzamide catalyzed by Pd-Schiff-Base@-Fe_3O_4MNPs are shown in Schemes 3 and 4, respectively, including full catalytic cycle including nucleophilic substitution and catalyst transformation.

4. Conclusion

Finally, we have presented a novel method for the synthesis of amide and 5-substituted 1*H*-tetrazole starting from halobenzene using $K_2[Ni(CN)_4]$ as safe inorganic cyanide source in presence of new type of magnetic nanocatalyst (Pd-Schiff-Base@Fe_3O_4MNPs) was synthesized from immobilization of palladium on functionalized Fe_3O_4 magnetic nanoparticles. The characterization data provided us adequate and useful data in order to propose the authentic structure. Further achieved results indicate stable and strong grafted palladium bonds to different sites of catalyst support.

Appendix A. Supplementary data

Supplementary data to this article can be found online at https://doi.org/10.1016/j.jorganchem.2018.11.006.

References

[1] K.C. Nicolaou, D.J. Edmonds, P.G. Bulger, Cascade reactions in total synthesis, Angew. Chem. Int. Ed. 45 (2006) 7134–7186.
[2] H. Pellissier, Asymmetric domino reactions. Part A: reactions based on the use of chiral auxiliaries, Tetrahedron 62 (2006) 1619–1665.
[3] H.-g. Peng, L. Xu, H. Wu, K. Zhang, P. Wu, One-pot synthesis of benzamide over a robust tandem catalyst based on center radially fibrous silica encapsulated TS-1, Chem. Commun. 49 (2013) 2709–2711.
[4] H. Fujiwara, Y. Ogasawara, K. Yamaguchi, N. Mizuno, A one-pot synthesis of primary amides from aldoximes or aldehydes in water in the presence of a supported rhodium catalyst, Angew. Chem. 119 (2007) 5294–5297.
[5] R.J. Herr, 5-Substituted-1H-tetrazoles as carboxylic acid isosteres: medicinal chemistry and synthetic methods, Biorg. Med. Chem. 10 (2002) 3379–3393.
[6] G.F. Holland, J.N. Pereira, Heterocyclic tetrazoles, a new class of lipolysis inhibitors, J. Med. Chem. 10 (1967) 149–154.
[7] V.A. Ostrovskii, R.E. Trifonov, E.A. Popova, Medicinal chemistry of tetrazoles, Russ. Chem. Bull. 61 (2012) 768–780.
[8] A. Nohara, H. Kuriki, T. Saijo, H. Sugihara, M. Kanno, Y. Sanno, Studies on antianaphylactic agents. 5. Synthesis of 3-(1H-tetrazol-5-yl)chromones, a new series of antiallergic substances, J. Med. Chem. 20 (1977) 141–145.
[9] A. Andrus, B. Partridge, J.V. Heck, B.G. Christensen, The synthesis of N-(tetrazol-5-yl)azetidin-2-ones, Tetrahedron Lett. 25 (1984) 911–914.
[10] Y. Momose, T. Maekawa, H. Odaka, H. Ikeda, T. Sohda, Novel 5-substituted-1H-tetrazole derivatives as potent glucose and lipid lowering agents, Chem. Pharm. Bull. 50 (2002) 100–111.
[11] S. Wu, A. Fluxe, J. Sheffer, J.M. Janusz, B.E. Blass, R. White, C. Jackson, R. Hedges, M. Murawsky, B. Fang, Discovery and in vitro/in vivo studies of tetrazole derivatives as Kv1. 5 blockers, Bioorg. Med. Chem. Lett 16 (2006) 6213–6218.
[12] L. Myznikov, A. Hrabalek, G. Koldobskii, Drugs in the tetrazole series.(Review), Chem. Heterocycl. Comp. 43 (2007) 1–9.
[13] M.J. Schocken, R.W. Creekmore, G. Theodoridis, G.J. Nystrom, R.A. Robinson, Microbial transformation of the tetrazolinone herbicide F5231, Appl. Environ. Microbiol. 55 (1989) 1220–1222.
[14] A.N. Chermahini, A. Teimouri, F. Momenbeik, A. Zarei, Z. Dalirnasab, A. Ghaedi, M. Roosta, Clay-catalyzed synthesis of 5-substituent 1-H-tetrazoles, J. Heterocycl. Chem. 47 (2010) 913–922.
[15] D.R. Patil, M.B. Deshmukh, D.S. Dalal, Ammonium acetate mediated synthesis of 5-substituted 1H-tetrazoles, J. Iran. Chem. Soc. 9 (2012) 799–803.
[16] D. Amantini, R. Beleggia, F. Fringuelli, F. Pizzo, L. Vaccaro, TBAF-catalyzed synthesis of 5-substituted 1 H-tetrazoles under solventless conditions, J. Org. Chem. 69 (2004) 2896–2898.
[17] B. Gutmann, J.P. Roduit, D. Roberge, C.O. Kappe, Synthesis of 5-substituted 1H-tetrazoles from nitriles and hydrazoic acid by using a safe and scalable high-temperature microreactor approach, Angew. Chem. Int. Ed. 49 (2010) 7101–7105.
[18] W.G. Finnegan, R.A. Henry, R. Lofquist, An improved synthesis of 5-substituted

tetrazoles, J. Am. Chem. Soc. 80 (1958) 3908–3911.
[19] E. Lieber, T. Enkoji, Synthesis and properties of 5-(substituted) Mercaptotetrazoles1, J. Org. Chem. 26 (1961) 4472–4479.
[20] J.-J. Shie, J.-M. Fang, Microwave-assisted one-pot tandem reactions for direct conversion of primary alcohols and aldehydes to triazines and tetrazoles in aqueous media, J. Org. Chem. 72 (2007) 3141–3144.
[21] A. Kumar, R. Narayanan, H. Shechter, Rearrangement reactions of (hydroxyphenyl) carbenes, J. Org. Chem. 61 (1996) 4462–4465.
[22] D.P. Matthews, J.E. Green, A.J. Shuker, Parallel synthesis of alkyl tetrazole derivatives using solid support chemistry, J. Comb. Chem. 2 (2000) 19–23.
[23] T. Jin, F. Kitahara, S. Kamijo, Y. Yamamoto, Copper-catalyzed synthesis of 5-substituted 1H-tetrazoles via the [3+2] cycloaddition of nitriles and trimethylsilyl azide, Tetrahedron Lett. 49 (2008) 2824–2827.
[24] M. Lakshmi Kantam, K. Kumar, C. Sridhar, Nanocrystalline ZnO as an efficient heterogeneous catalyst for the synthesis of 5-substituted 1H-tetrazoles, Adv. Synth. Catal. 347 (2005) 1212–1214.
[25] A.N. Chermahini, A. Teimouri, A. Moaddeli, Simple and efficient synthesis of 5-substituted 1-H-tetrazoles using metal-modified clay catalysts, Heteroat. Chem. 22 (2011) 168–173.
[26] M. Kazemi, L. Shiri, H. Kohzadi, Recent advances in aryl alkyl and dialkyl sulfide synthesis, Phosphorus, Sulfur, Silicon Relat. Elem. 190 (2015) 978–1003.
[27] M. Sheykhan, L. Ma'mani, A. Ebrahimi, A. Heydari, Sulfamic acid heterogenized on hydroxyapatite-encapsulated γ-Fe2O3 nanoparticles as a magnetic green interphase catalyst, J. Mol. Catal. Chem. 335 (2011) 253–261.
[28] N.A. Frey, S. Peng, K. Cheng, S. Sun, Magnetic nanoparticles: synthesis, functionalization, and applications in bioimaging and magnetic energy storage, Chem. Soc. Rev. 38 (2009) 2532–2542.
[29] Y. Min, M. Akbulut, K. Kristiansen, Y. Golan, J. Israelachvili, The role of interparticle and external forces in nanoparticle assembly, Nat. Mater. 7 (2008) 527–538.
[30] D. Astruc, F. Lu, J.R. Aranzaes, Nanoparticles as recyclable catalysts: the frontier between homogeneous and heterogeneous catalysis, Angew. Chem. Int. Ed. 44 (2005) 7852–7872.
[31] J.-P. Jolivet, S. Cassaignon, C. Chanéac, D. Chiche, O. Durupthy, D. Portehault, Design of metal oxide nanoparticles: control of size, shape, crystalline structure and functionalization by aqueous chemistry, Compt. Rendus Chem. 13 (2010) 40–51.
[32] L. Shiri, A. Ghorbani-Choghamarani, M. Kazemi, Sulfides synthesis: nanocatalysts in C–S cross-coupling reactions, Aust. J. Chem. 69 (2016) 585–600.
[33] L. Shiri, A. Ghorbani-Choghamarani, M. Kazemi, Synthesis and characterization of tribenzyl ammonium-tribromide supported on magnetic Fe3O4 nanoparticles: a robust magnetically recoverable catalyst for the oxidative coupling of thiols and oxidation of sulfides, Res. Chem. Intermed. (2016) 1–18.
[34] S. Laurent, D. Forge, M. Port, A. Roch, C. Robic, L. Vander Elst, R.N. Muller, Magnetic iron oxide nanoparticles: synthesis, stabilization, vectorization, physicochemical characterizations, and biological applications, Chem. Rev. 108 (2008) 2064–2110.
[35] M. Hasanzadeh, N. Shadjou, E. Omidinia, Mesoporous silica (MCM-41)-Fe< sub> 2 O< sub> 3 as a novel magnetic nanosensor for determination of trace amounts of amino acids, Colloids Surfaces B Biointerfaces 108 (2013) 52–59.
[36] M. Mahmoudi, S. Sant, B. Wang, S. Laurent, T. Sen, Superparamagnetic iron oxide nanoparticles (SPIONs): development, surface modification and applications in chemotherapy, Adv. Drug Deliv. Rev. 63 (2011) 24–46.
[37] B. Wang, Q. Wei, S. Qu, Synthesis and characterization of uniform and crystalline magnetite nanoparticles via oxidation-precipitation and modified co-precipitation methods, Int. J. Electrochem. Sci 8 (2013) 3786–3793.
[38] C. Graf, D.L. Vossen, A. Imhof, A. van Blaaderen, A general method to coat colloidal particles with silica, Langmuir 19 (2003) 6693–6700.
[39] P. Tartaj, T. González-Carreño, C.J. Serna, Synthesis of nanomagnets dispersed in colloidal silica cages with applications in chemical separation, Langmuir 18 (2002) 4556–4558.
[40] P. Tartaj, C.J. Serna, Synthesis of monodisperse superparamagnetic Fe/silica nanospherical composites, J. Am. Chem. Soc. 125 (2003) 15754–15755.
[41] L. Lei, X. Liu, Y. Li, Y. Cui, Y. Yang, G. Qin, Study on synthesis of poly(GMA)-grafted Fe3O4/SiOX magnetic nanoparticles using atom transfer radical polymerization and their application for lipase immobilization, Mater. Chem. Phys. 125 (2011) 866–871.
[42] K.G. Hu, L. Neoh, E. Cen, T. Kang, Cellular response to magnetic nanoparticles "PEGylated" via surface-initiated atom transfer radical polymerization, Biomacromolecules 7 (2006) 809–816.
[43] A.R. Herdt, B.-S. Kim, T.A. Taton, Encapsulated magnetic nanoparticles as supports for proteins and recyclable biocatalysts, Bioconjug. Chem. 18 (2007) 183–189.
[44] S.S.A. Darbandizadeh Mohammad Abadi, M.A. Karimi Zarchi, A novel route for the synthesis of 5-substituted 1-H tetrazoles in the presence of polymer-supported palladium nanoparticles, New J. Chem. 41 (2017) 10397–10406.
[45] M.A.K. Zarchi, S.S.A.D.M. Abadi, Synthesis of a polymer-capped palladium nanoparticles and its application as a reusable catalyst in oxidative coupling reaction of α-hydroxyketones and 1,2-diamines for preparation of pyrazines and quinoxalines, J. Iran. Chem. Soc. 15 (2018) 915–929.
[46] Z. Zhang, H. Duan, S. Li, Y. Lin, Assembly of magnetic nanospheres into one-dimensional nanostructured carbon hybrid materials, Langmuir 26 (2010) 6676–6680.
[47] A.-H. Lu, W.-C. Li, N. Matoussevitch, B. Spliethoff, H. Bonnemann, F. Schuth, Highly stable carbon-protected cobalt nanoparticles and graphite shells, Chem. Commun. (2005) 98–100.
[48] L. Wang, J. Luo, M.M. Maye, Q. Fan, Q. Rendeng, M.H. Engelhard, C. Wang, Y. Lin, C.-J. Zhong, Iron oxide-gold core-shell nanoparticles and thin film assembly, J. Mater. Chem. 15 (2005) 1821–1832.
[49] Y. Lee, M.A. Garcia, N.A. Frey Huls, S. Sun, Synthetic tuning of the catalytic properties of Au-Fe3O4 nanoparticles, Angew. Chem. 122 (2010) 1293–1296.
[50] M. Esmaeilpour, A.R. Sardarian, J. Javidi, Schiff base complex of metal ions supported on superparamagnetic Fe3O4@SiO2 nanoparticles: an efficient, selective and recyclable catalyst for synthesis of 1,1-diacetates from aldehydes under solvent-free conditions, Appl. Catal. Gen. 445–446 (2012) 359–367.
[51] D. Wang, D. Astruc, Fast-growing field of magnetically recyclable nanocatalysts, Chem. Rev. 114 (2014) 6949–6985.
[52] C.W. Lim, I.S. Lee, Magnetically recyclable nanocatalyst systems for the organic reactions, Nano Today 5 (2010) 412–434.
[53] Y. Wang, J. Luo, Z. Liu, Salicylaldoxime-functionalized poly(ethylene glycol)-bridged dicationic ionic liquid ([salox-PEG1000-DIL][BF4]) as a novel ligand for palladium-catalyzed Suzuki–Miyaura reaction in water, Appl. Organomet. Chem. 27 (2013) 601–605.
[54] F. Havasi, A. Ghorbani-Choghamarani, F. Nikpour, Pd-grafted functionalized mesoporous MCM-41: a novel, green and heterogeneous nanocatalyst for the selective synthesis of phenols and anilines from arylhalides in water, New J. Chem. 39 (2015) 6504–6512.
[55] S.S.A. Darbandizadeh Mohammad Abadi, M. Abdollahi-Alibeik, Fe3O4@FeSO4-MCM-41 nanoparticles and reusable catalyst for the synthesis of quinoxalines in solvent-free conditions, Siliconindia 10 (2018) 1667–1678.
[56] S. Ghosh, A.Z.M. Badruddoza, M.S. Uddin, K. Hidajat, Adsorption of chiral aromatic amino acids onto carboxymethyl-β-cyclodextrin bonded Fe3O4/SiO2 core–shell nanoparticles, J. Colloid Interface Sci. 354 (2011) 483–492.
[57] M. Hajjami, B. Tahmasbi, Synthesis and characterization of glucosulfonic acid supported on Fe3O4 nanoparticles as a novel and magnetically recoverable nanocatalyst and its application in the synthesis of polyhydroquinoline and 2,3-dihydroquinazolin-4(1H)-one derivatives, RSC Adv. 5 (2015) 59194–59203.
[58] L. Shiri, A. Ghorbani-Choghamarani, M. Kazemi, Cu(II) immobilized on Fe3O4–diethylenetriamine: a new magnetically recoverable catalyst for the synthesis of 2,3-dihydroquinazolin-4(1H)-ones and oxidative coupling of thiols, Appl. Organomet. Chem. 31 (5) (2016), e3596. https://onlinelibrary.wiley.com/doi/abs/10.1002/aoc.3596.
[59] X.-N. Zhao, H.-C. Hu, F.-J. Zhang, Z.-H. Zhang, Magnetic CoFe 2 O 4 nanoparticle immobilized N-propyl diethylenetriamine sulfamic acid as an efficient and recyclable catalyst for the synthesis of amides via the Ritter reaction, Appl. Catal. Gen. 482 (2014) 258–265.
[60] M. Navidi, B. Movassagh, S. Rayati, Multi-walled carbon nanotubes functionalized with a palladium (II)-Schiff base complex: a recyclable and heterogeneous catalyst for the copper-, phosphorous-and solvent-free synthesis of ynones, Appl. Catal. Gen. 452 (2013) 24–28.
[61] M. Gholinejad, M. Seyedhamzeh, M. Razeghi, C. Najera, M. Kompany-Zareh, Iron oxide nanoparticles modified with carbon quantum nanodots for the stabilization of palladium nanoparticles: an efficient catalyst for the suzuki reaction in aqueous media under mild conditions, ChemCatChem 8 (2016) 441–447.
[62] Z.-S. Wu, S. Yang, Y. Sun, K. Parvez, X. Feng, K. Müllen, 3D nitrogen-doped graphene aerogel-supported Fe3O4 nanoparticles as efficient electrocatalysts for the oxygen reduction reaction, J. Am. Chem. Soc. 134 (2012) 9082–9085.
[63] G. Du, Z. Liu, X. Xia, Q. Chu, S. Zhang, Characterization and application of Fe3O4/SiO2 nanocomposites, J. Sol. Gel Sci. Technol. 39 (2006) 285–291.
[64] H.-Y. Xie, R. Zhen, B. Wang, Y.-J. Feng, P. Chen, J. Hao, Fe3O4/Au Core/Shell nanoparticles modified with Ni2+– Nitrilotriacetic acid specific to histidine-tagged proteins, J. Phys. Chem. C 114 (2010) 4825–4830.
[65] G. Wang, Z. Gao, G. Wan, S. Lin, P. Yang, Y. Qin, High densities of magnetic nanoparticles supported on graphene fabricated by atomic layer deposition and their use as efficient synergistic microwave absorbers, Nano Research 7 (2014) 704.
[66] J. Mu, B. Chen, Z. Guo, M. Zhang, Z. Zhang, P. Zhang, C. Shao, Y. Liu, Highly dispersed Fe 3 O 4 nanosheets on one-dimensional carbon nanofibers: synthesis, formation mechanism, and electrochemical performance as supercapacitor electrode materials, Nanoscale 3 (2011) 5034–5040.
[67] I. Fanlo, F. Gervilla, E. Mateo, S. Irusta, X-ray photoelectron spectroscopy characterization of natural chromite from Mercedita Mine (Eastern Cuba): quantification of the Fe3+/Fe2+ ratio, Eur. J. Mineral 20 (2008) 125–129.
[68] D. Marton, K. Boyd, A. Al-Bayati, S. Todorov, J. Rabalais, Carbon nitride deposited using energetic species: a two-phase system, Phys. Rev. Lett. 73 (1994) 118.
[69] C. Ronning, H. Feldermann, R. Merk, H. Hofsäss, P. Reinke, J.-U. Thiele, Carbon nitride deposited using energetic species: a review on XPS studies, Phys. Rev. B 58 (1998) 2207.
[70] Y. Mao, H. Duan, B. Xu, L. Zhang, Y. Hu, C. Zhao, Z. Wang, L. Chen, Y. Yang,

Lithium storage in nitrogen-rich mesoporous carbon materials, Energy Environ. Sci. 5 (2012) 7950–7955.
[71] F. Han, L. Ma, Q. Sun, C. Lei, A. Lu, Rationally designed carbon-coated Fe3O4 coaxial nanotubes with hierarchical porosity as high-rate anodes for lithium ion batteries, Nano Research 7 (2014) 1706–1717.
[72] H.M. Hassan, E.M. Saad, M.S. Soltan, M.A. Betiha, I.S. Butler, S.I. Mostafa, A palladium (II) 4-hydroxysalicylidene Schiff-base complex anchored on functionalized MCM-41: an efficient heterogeneous catalyst for the epoxidation of olefins, Appl. Catal. Gen. 488 (2014) 148–159.
[73] R. Li, P. Zhang, Y. Huang, P. Zhang, H. Zhong, Q. Chen, Pd–Fe 3 O 4@ C hybrid nanoparticles: preparation, characterization, and their high catalytic activity toward Suzuki coupling reactions, J. Mater. Chem. 22 (2012) 22750–22755.
[74] A. Ghorbani-Choghamarani, P. Moradi, B. Tahmasbi, Ni-S-methylisothiourea complexes supported on boehmite nanoparticles and their application in the synthesis of 5-substituted tetrazoles, RSC Adv. 6 (2016) 56638–56646.
[75] B.S. Jursic, B.W. Leblanc, Preparation of tetrazoles from organic nitriles and sodium azide in micellar media, J. Heterocycl. Chem. 35 (1998) 405–408.
[76] P. Moradi, A. Ghorbani-Choghamarani, Efficient synthesis of 5-substituted tetrazoles catalysed by palladium-S-methylisothiourea complex supported on boehmite nanoparticles, Appl. Organomet. Chem. 31 (2016) 922–928.